



저작자표시-비영리-동일조건변경허락 2.0 대한민국

이용자는 아래의 조건을 따르는 경우에 한하여 자유롭게

- 이 저작물을 복제, 배포, 전송, 전시, 공연 및 방송할 수 있습니다.
- 이차적 저작물을 작성할 수 있습니다.

다음과 같은 조건을 따라야 합니다:



저작자표시. 귀하는 원저작자를 표시하여야 합니다.



비영리. 귀하는 이 저작물을 영리 목적으로 이용할 수 없습니다.



동일조건변경허락. 귀하가 이 저작물을 개작, 변형 또는 가공했을 경우에는, 이 저작물과 동일한 이용허락조건하에서만 배포할 수 있습니다.

- 귀하는, 이 저작물의 재이용이나 배포의 경우, 이 저작물에 적용된 이용허락조건을 명확하게 나타내어야 합니다.
- 저작권자로부터 별도의 허가를 받으면 이러한 조건들은 적용되지 않습니다.

저작권법에 따른 이용자의 권리는 위의 내용에 의하여 영향을 받지 않습니다.

이것은 [이용허락규약\(Legal Code\)](#)을 이해하기 쉽게 요약한 것입니다.

[Disclaimer](#)

Thesis for the degree of
Doctor of Philosophy

A Study on Structural Optimization of Refrigerator Inner Case Considering Thermal Deformation



February 2011

The Graduate School
Korea Maritime University

School of Mechanical Engineering

Jian Guang Zhai

Contents

Abstract.....	i
List of Figures.....	iv
List of Tables	viii
Chapter 1 Introduction	1
1.1 Research Background	1
1.2 Research Content and Objective.....	4
Chapter 2 FEM Application in Refrigerator Structural Analysis	5
2.1 FEM Application in Refrigerator.....	5
2.2 Thermal Deformation Analysis of Refrigerator	7
2.3 Structural Analysis Process.....	19
2.4 Analysis Results and Discussion	21
Chapter 3 Structural Optimization of refrigerator	27
3.1 Introduction	27
3.2 Parametric Modeling.....	28
3.3 Structural Optimization Using FEM.....	34
3.4 Structural Optimization Using Artificial Neural Networks and Genetic Algorithm	53
Chapter 4 New Design Concept of Refrigerator to Decrease Thermal Deformation.....	75
4.1 Introduction	75
4.2 Diamond Pattern Design	75
4.3 Pre-Forming Design	88
Chapter 5 Conclusion	96
Acknowledgements	100

Reference	101
Appendix: Visual Basic Code	106
Publications	121



A Study on Structural Optimization of Refrigerator Inner Case Considering Thermal Deformation

Jian Guang Zhai

Department of Mechanical Engineering

Graduate School of

Korea Maritime University

Abstract

In refrigerator constructions where in-situ foamed polyurethane thermal insulation material is employed, the structural rigidity of refrigerator cabinet is generated by foaming process which the polyurethane is solidified and hardened after injection of the foam reactant. However, the outer case may be made of steel and the inner liner of plastics. The three materials which possess different thermal properties will produce different thermal deformation and great stresses during the foaming process and subsequent operating process.

In this paper, the Finite Element Method (FEM) is applied to calculate thermal deformation of specified refrigerator model. The sequential thermo-mechanical coupling analysis in ANSYS software was also used in this study. Firstly, the constant temperature field was obtained by applying heat transfer coefficients on the refrigerator FE model, then, in the thermo-mechanical deformation analysis process, thermal analysis units were changed into structural analysis units and the mechanical field was analyzed proceeding from an already known temperature field. The finite element model was comprised of solid

elements and shell elements. The foam part was meshed with solid-70 element in the thermal analysis and solid-185 element in the mechanical analysis respectively. The plastic liners and all sheet metal components were meshed with the shell-63 element.

In order to make a series of analysis of refrigerator models, we developed a method of numerical analysis based on a combination of VB 6.0 and the ANSYS Parametric Design Language (APDL). A convenient interface for parameter input was developed and thermo-mechanical analysis procedure could be carried out using a VB interface by realizing seamless integration of the two pieces of software and increasing analysis efficiency.

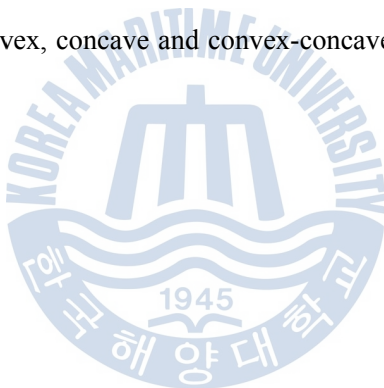
However, we wanted to figure out the effect of plaque parameters, which have obvious effects on decreasing thermally induced cabinet bowing deformation, including plaque depth, plaque width, interval distance between plaques, and plaque numbers using a designated distance of inner case sidewall. In this study, the plaques were designed within a designated distance of 740mm. We firstly analyzed the effect of variables of plaque depth, width and numbers on refrigerator thermal deformation. Then, with designated numbers, we analyzed the effect of plaque depth, width and interval distance.

In chapter 3, we also used a method called the BP-GA method to obtain the optimal plaque parameters for minimum refrigerator inner case deformation. The training data were obtained by FEM model utilizing ANSYS because of lack of the experimental data. A total of forty-five FEM models were analyzed among which twenty-five models were arranged by the orthogonal test method according to the plaque's depth (D), width (W) and interval distance (S). The FEM analysis results of thirty-eight models were inputted as training data and the other seven were taken as test data after the BP network training process in order to know how perfect the predicting model obtained by ANN training would match with the actual FEM analysis results.

In chapter 4, the inner case was designed into a diamond shape so that bad

appearances were anticipated to be avoided after foaming. We designed several models with a diamond shape in a hexagonal pyramid style on the inner case wall in order to analyze the cooling effect and thermal deformation. And the diamond pattern was designed separately in convex style and concave style. We took thermo-mechanical analysis of the diamond shape inner liner.

Based on the above mentioned analysis results, we came up with the concept of pre-forming. According to the inward bowing characteristic of thermal deformation, we pre-formed the sidewall by a reverse shape deformation to some suitable extent. The pre-formed area was designed to be in the central part of the inner liner area. The normal thermal deformation was found to be about five millimeter for the refrigerator model in this study. We designed convex, concave and convex-concave pre-formed models at three millimeter.



List of Figures

- Fig. 1 Refrigerator model
- Fig. 2 Plaques on sidewall of freezer inner case
- Fig. 3 Refrigerator component with plaques
- Fig. 4 FE model for cabinet
- Fig. 5 Analysis condition
- Fig. 6 Flow chart of thermal analysis
- Fig. 7 Flow chart of structural analysis
- Fig. 8 Temperature distribution of model-D0
- Fig. 9 Temperature distribution of model-D1
- Fig. 10 X-displacement of model-D0
- Fig. 11 X-displacement at middle cross section
- Fig. 12 X-displacement of model-D1
- Fig. 13 X-displacement of model-D2
- Fig. 14 X-displacement of model-D3
- Fig. 15 X-displacement of model-D4
- Fig. 16 Comparison of structural analysis results
- Fig. 17 Parameters on side view
- Fig. 18 Parameters on front view
- Fig. 19 Parametric modeling process
- Fig. 20 Flow chart of parametric modeling
- Fig. 21 Optimization analysis process
- Fig. 22 Iteration process of N
- Fig. 23 Iteration process of Q and $DMAX$

Fig. 24 Iteration process of W

Fig. 25 Iteration process of Q and $DMAX$ (N=6)

Fig. 26 Iteration process of W and S (N=6)

Fig. 27 Iteration process of Q and $DMAX$ (N=8)

Fig. 28 Iteration process of W and S (N=8)

Fig. 29 Iteration process of Q and $DMAX$ (N=10)

Fig. 30 Iteration process of W and S (N=10)

Fig. 31 Iteration process of Q and $DMAX$ (N=12)

Fig. 32 Iteration process of W and S (N=12)

Fig. 33 Iteration process of Q and $DMAX$ (N=14)

Fig. 34 Iteration process of W and S (N=14)

Fig. 35 Iteration process of Q and $DMAX$ (N=16)

Fig. 36 Iteration process of W and S (N=16)

Fig. 37 Iteration process of Q and $DMAX$ (N=18)

Fig. 38 Iteration process of W and S (N=18)

Fig. 39 Parametric analysis interface based on VB 6.0

Fig. 40 BP network constitution

Fig. 41 Function of tan-sigmoid activation

Fig. 42 Function of linear activation

Fig. 43 The ANN structure

Fig. 44 GA process

Fig. 45 Result of GA optimization analysis

Fig. 46 FEM analysis result with GA optimization parameters

Fig. 47 MAX deformation of model with plaques

Fig. 48 MAX deformation of model without plaques

Fig. 49 Diamond geometry

Fig. 50 Convex diamond

Fig. 51 Concave diamond

Fig. 52 Diamond area

Fig. 53 Pattern_5

Fig. 54 Plaque model (Depth: 1mm)

Fig. 55 Temperature condition of smooth model

Fig. 56 Temperature condition of pattern_1

Fig. 57 Temperature condition of pattern_2

Fig. 58 Temperature condition of pattern_3

Fig. 59 Temperature condition of pattern_4

Fig. 60 Temperature condition of pattern_5

Fig. 61 Temperature condition of plaque model

Fig. 62 Structural analysis result smooth model

Fig. 63 Structural analysis result of pattern_1

Fig. 64 Structural analysis result of pattern_2

Fig. 65 Structural analysis result of pattern_3

Fig. 66 Structural analysis result of pattern_4

Fig. 67 Structural analysis result of pattern_5

Fig. 68 Structural analysis result of plaque pattern

Fig. 69 Pre-forming area

Fig. 70 Pre-forming of convex pattern

Fig. 71 Pre-forming of concave pattern

Fig. 72 Pre-forming of convex-concave pattern (A-A section)

Fig. 73 Temperature distribution of smooth model

Fig. 74 Temperature distribution of convex model

Fig. 75 Temperature distribution of concave model

Fig. 76 Temperature distribution of convex-concave model

Fig. 77 Structural analysis result of smooth model

Fig. 78 Actual deformation of convex model

Fig. 79 Actual deformation of concave model

Fig. 80 Actual deformation of convex-concave model



List of Tables

Table 1	Distance between plaques
Table 2	FEM models
Table 3	Material property
Table 4	Parameters for analysis
Table 5	Equivalent convective heat transfer coefficient
Table 6	Structural analysis results
Table 7	Geometry parameters of refrigerator model
Table 8	Plaque parameters
Table 9	Interval distance with different plaque numbers
Table 10	Optimization analysis result (N is variable)
Table 11	Analysis result (N=6)
Table 12	Analysis result (N=8)
Table 13	Analysis result (N=10)
Table 14	Analysis result (N=12)
Table 15	Analysis result (N=14)
Table 16	Analysis result (N=16)
Table 17	Analysis result (N=18)
Table 18	Factors and levels of orthogonal test
Table 19	Orthogonal test data
Table 20	Additional test data
Table 21	Data for testing BP network
Table 22	Test result

Table 23 FEM and GA optimization result

Table 24 Parameters of diamond models

Table 25 The lowest temperature of models

Table 26 Structural analysis result comparison of diamond models

Table 27 Analysis results of pre-forming models



Chapter 1 Introduction

1.1 Research Background

Since 1927 when General Electric introduced the Monitor Refrigerator refrigerators onto the market, refrigerators have been widely used all through the world. Today refrigerators can be found in 99.5% of homes around the world. The primary refrigerator structure is a sandwich of steel on the outer surface, a foam core and plastic inner liners. The outer steel plate is comprised of a wrapper with roll-formed front and rear flanges, corner bracket reinforcements, a back panel and a deck ^[1]. The inner liners are made from thermoformed high impact acrylonitrile-butadiene-styrene (ABS) and form the freezer compartment and the refrigerator compartment. The inner and outer layers adhere to the polyurethane foam core. However, over deflection of freezer inner case would also occur now and again under extreme test or operating conditions, which would lead to rack dropping or even cracking of the inner liner. The main reason is thermal deformation of the inner case under large temperature difference and different material properties. More recently, as refrigerator case structure become more and more large and complicated, it is easier to cause cracks during storage process or under operating conditions than before. The reason for the cracking is very complicated; however, the main reason is the different thermal properties of the composite inner case materials under the great temperature differences.

Although engineers have figured out various methods to reduce the inner case deformation and stress for the purpose of avoiding inner cracks, few theoretic research reports for avoiding refrigerator inner case cracks can be found in the world. Usually, engineers would rather design a lot of experiments of different refrigerator models in order

to obtain an optimal structure with little inner case deformation, which would cause a great waste of money and research and development (R&D) time. Consequently, there is a need for a tool that would make the evaluation of a refrigerator structure available for engineers during the R&D process

In order to decrease thermal bowing deformation, usually stiffening beams are inserted into the refrigerator cabinet, or insert middle layer between inner liner and polyurethane thermal insulation material, which inevitably increases the cost of manufacture. Until now, there haven't been any effective technical measures reported to settle such problems. Usually, the traditional refrigerator inner liner is designed into a smooth surface for an aesthetics purpose. However, as we all know rough surfaces contribute to increasing heat transfer area, and air flow resistance. If the height of the rough unit is beyond of that of the laminar layer, the heat transfer coefficient will also increase because of the disturbance effect. And, the rough surface will also increase structural rigidity of the inner liner and resist thermal bowing. So, a rough surface is better than a smooth surface to increase the heat transfer effect and structural rigidity ^[2].

In the past, worldwide refrigerator manufacture industries usually required that engineers build and test several prototypes, with results then compared them with the current production cabinets for developing new techniques. This trial-and-error approach is costly and time-consuming, leading to only incremental changes. Recently, the companies have enjoyed more substantial benefits from an approach that utilizes leading-edge simulation combined with experimental tools to assess complex structural behavior, for example, Whirlpool, LG, etc. FEM is the most popular way to simulate and take refrigerator thermal and mechanical analysis. Engineers construct a FEM model of the cabinet using solid and shell elements. By using ANSYS Mechanical software, we can take thermo-mechanical analysis and structural optimization analysis of the refrigerator ^[3~8].

In ANSYS, there are two fundamentally different types of optimization. One is

referred to as design optimization, the other is a technique known as topological optimization. For the design optimization, the ANSYS optimization routines employ three types of variables that characterize the design process: design variables, state variables, and the objective function ^[3]. Once the design variables, constraints, objectives, and the relationships between them have been chosen, the problem can be expressed in the following form:

Find x that minimizes $F(x)$

Subject to $g(x) \leq 0$, $h(x) = 0$ and $x_{lb} \leq x \leq x_{ub}$

Where F is an objective, x is a vector of design variables, g is a vector of inequality constraints, h is a vector of equality constraints, and x_{lb} , x_{ub} are vectors of lower and upper bounds on the design variables. Maximization problems can be converted to minimization problems by multiplying the objective by -1. Constraints can be reversed in a similar manner. Equality constraints can be replaced by two inequality constraints.

During recent years, simulated annealing, genetic algorithms, and neural network methods represent a new class of mathematical programming techniques that have come into prominence over the last decade. Simulated annealing is analogous to the physical process of annealing of solids. The genetic algorithms are search techniques based on the mechanics of natural selection and natural genetics. Neural network methods are based on solving the problem using the efficient computing power of the network of interconnected “neuron” processors.

1.2 Research Content and Objective

In this paper, we designed refrigerator FE models trying to take thermo-structural analysis instead of by experiment. We analyzed models with plaques on the inner case comparing to models with a smooth surface. The plaques contributed to increasing surface roughness and rigidity so that thermal bowing deformation could be decreased. However, the plaque parameters such as plaque depth, plaque width, plaque numbers and interval distance between plaques have different effects on decreasing refrigerator thermal deformation. We aimed to obtain the optimal plaque parameters for the given refrigerator models and to figure out the relationship between plaque parameters and refrigerator thermal bowing deformation by taking structural optimization. We also tried to set up a parametric analysis interface in order to efficiently obtain many analysis data which were needed as input in the optimization analysis process instead of repeating the same artificial modeling and loading processes. However, we could not obtain the explicit expressions for the relationship between plaque parameters and refrigerator deformation after taking optimization analysis in ANSYS. And we were also not so sure about the FEM analysis result errors using traditional calculating methods in ANSYS. We tried to take optimization using the popular GA method comparing to FEM analysis results and we were able to obtain explicit expression by utilizing the BP neural network.

Based on the previous heat transfer theory and analysis results, we tried to get some new mechanical design ideas not only for decreasing refrigerator thermal deformation, but also to improve refrigerator inner structure without increasing manufacture cost.

Chapter 2 FEM Application in Refrigerator Structural Analysis

2.1 FEM Application in Refrigerator

Refrigeration is the process of removing heat from an enclosed space, or from a substance to lower its temperature. A refrigerator uses the evaporation of a liquid to absorb heat. The liquid, or refrigerant, used in a refrigerator evaporates at an extremely low temperature, creating freezing temperatures inside the refrigerator. Global competition in the appliance industry is placing ever-increasing pressure on manufacturers to decrease costs while maintaining high quality. Refrigeration products are especially competitive, and as raw material costs for these appliances continue to rise, manufacturers are forced to take a close look at their product designs. The worldwide refrigerator manufacture companies have enjoyed more substantial benefits from an approach that utilizes leading-edge simulation, such as FEM, combined with experimental tools to assess complex structural behavior^[3].

Although the name of the finite element method was given recently, the concept dates back for centuries. Lord John William Strutt Rayleigh (late 1800s), developed a method for predicting the first natural frequency of simple structures^[4]. It assumed a deformed shape for a structure and then quantified this shape by minimizing the distributed energy in the structure. Walter Ritz then expanded this into a method, now known as the Rayleigh-Ritz method, for predicting the stress and displacement behavior of structures^[5]. In 1943, Richard Courant proposed breaking a continuous system into triangular segments^[6]. In the 1950s, a team from Boeing demonstrated that complex surfaces could be analyzed with a matrix of triangular shapes. Dr. Ray Clough coined the term “finite element” in 1960^[7,8]. The 1960s saw the true beginning of commercial FEA as digital computers replaced analog

ones with the capability of thousands of operations per second. In the early 1960s, the MacNeal-Schwendler Corporation (MSC) developed a general purpose FEA code. This original code had a limit of 68,000 degrees of freedom. When the NASA contract was complete, MSC continued development of its own version called MSC/NASTRAN^[9], while the original NASTRAN became available to the public and formed the basis of dozens of the FEA packages available today. Around the time MSC/NASTRAN was released, ANSYS, MARC, and SAP were introduced. By the 1970s, Computer-aided design, or CAD, was introduced later in the decade. In the 1980s, the use of FEA and CAD on the same workstation with developing geometry standards such as IGES and DXF permitted limited geometry transfer between the systems. In the 1980s, CAD progressed from a 2D drafting tool to a 3D surfacing tool, and then to 3D solid modeling system. Design engineers began to seriously consider incorporating FEA into the general product design process. As the 1990s came to an end, the PC platform had become a major force in high end analysis. The technology has become so accessible that it is actually being “hidden” inside CAD packages.

The basic ideas of the FEM as known today were presented in the papers of Turner, Clough, Martin and Topp^[10] and Argyris and Kelsey^[11]. The digital computer provided a rapid means of performing the many calculations involved in the finite element analysis and made the method practically viable.

2.2 Thermal Deformation Analysis of Refrigerator

2.2.1 Model Simplification

The primary refrigerator structure is a sandwich of steel on the outer surface, a foam core and plastic inner liners. The outer steel is comprised of a wrapper with roll-formed front and rear flanges, corner bracket reinforcements, a back panel and a deck. The inner liners are made from thermoformed high impact acrylonitrile-butadiene-styrene (ABS) and form the freezer compartment and the refrigerator compartment. The inner and outer layers adhere to the polyurethane foam core.

We should firstly simplify the refrigerator model in order to take analysis by finite element method in ANSYS. Some small structures such as screw holes, chamfer angles, etc were ignored in the FE model. The FE model is comprised of solid and shell elements. The foam part is meshed with solid-70 element in the thermal analysis and solid-185 element in the structural analysis. The plastic cases and all sheet metal components are meshed with shell-63 element. An extensive APDL input file was used to create the model with plaques. We used ANSYS V12.0 software and took a simplified FE modeling of a refrigerator, in which we didn't take into account any detail parts except for plaques. Fig.1 shows the refrigerator model with plaques. Fig. 2 shows the simplified model with plaques for the finite element method analysis. Fig.3 shows the component parts of the refrigerator inner case.

In this study, we made four plaques models with different plaque depth, and also a model with smooth inner case surface.

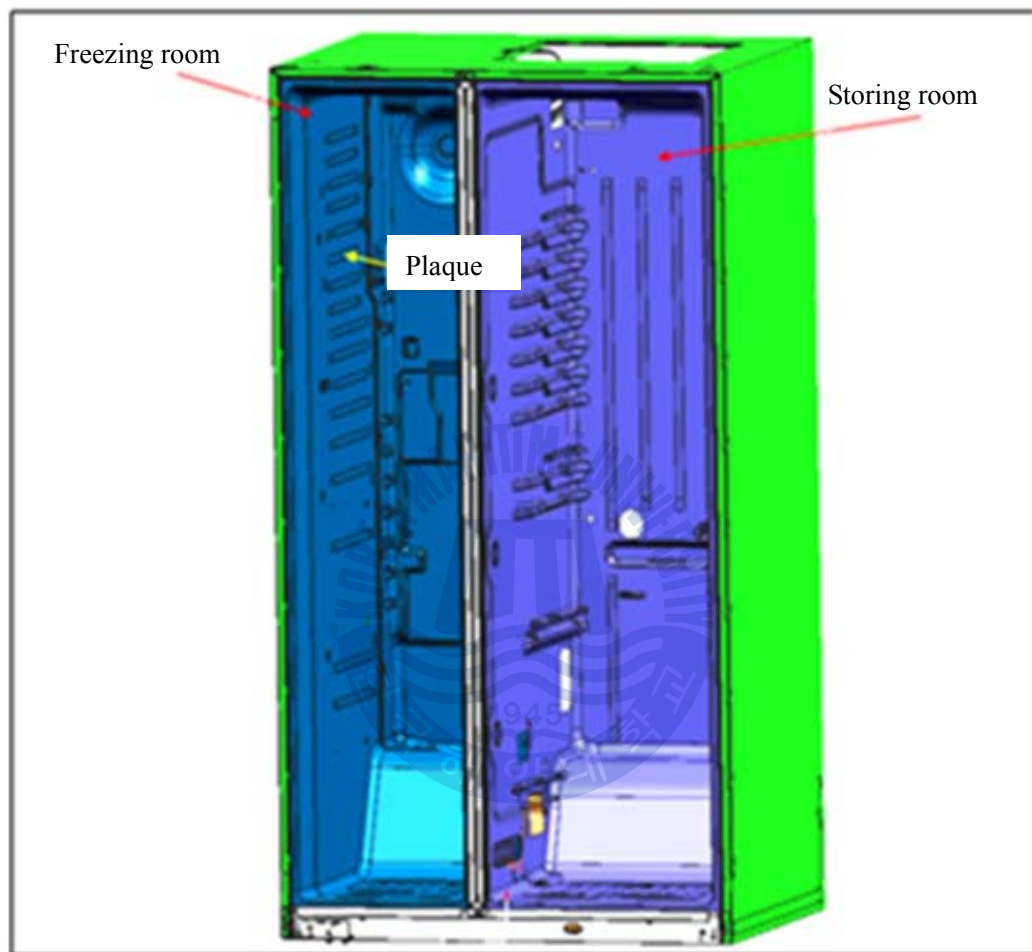


Fig. 1 Refrigerator model

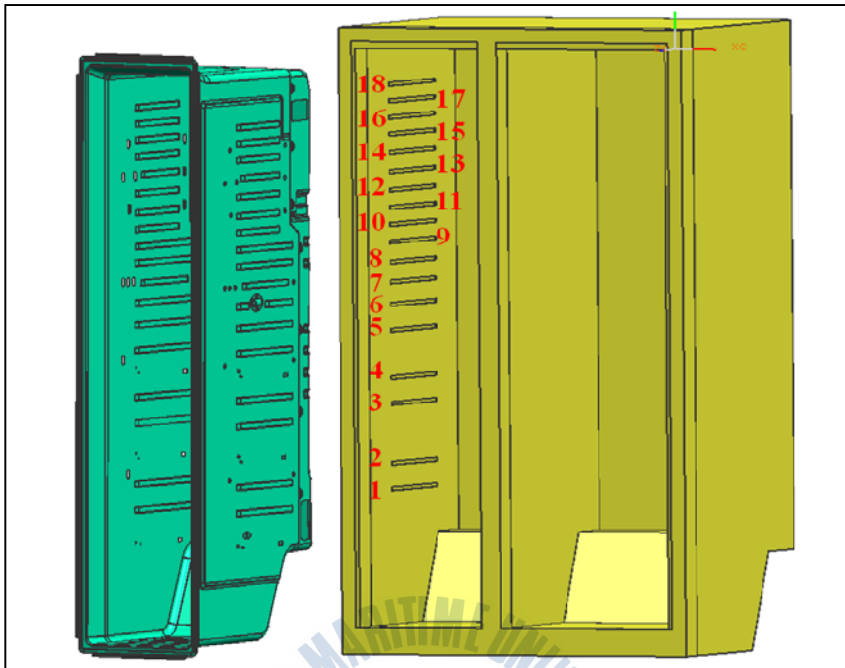


Fig. 2 Plaques on sidewall of freezer inner case

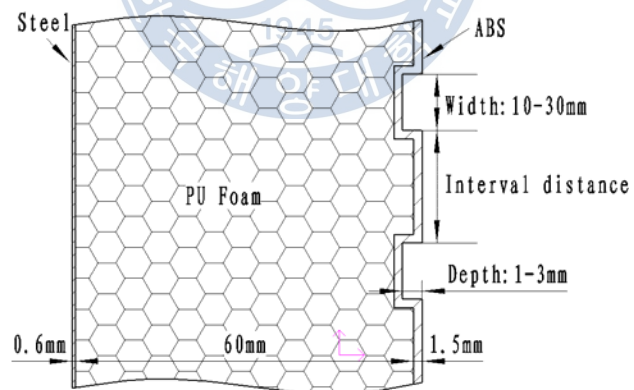


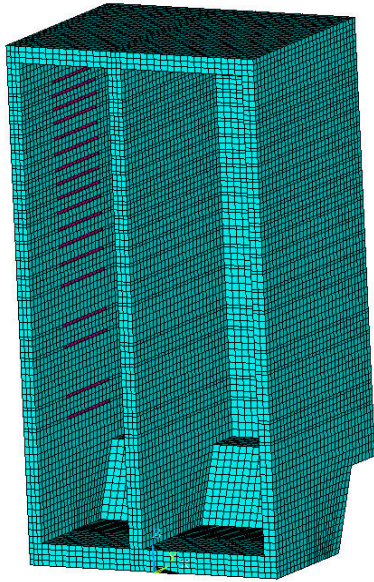
Fig. 3 Refrigerator component with plaques

Table 1 Distance between plaques

Number	Distance Between Plaques (mm)	Number	Distance Between Plaques (mm)
1-2	70	10-11	47
2-3	162	11-12	47
3-4	70	12-13	51
4-5	130	13-14	51
5-6	70	14-15	51
6-7	60	15-16	45
7-8	55	16-17	45
8-9	55	17-18	45
9-10	47		

Table 2 FEM models

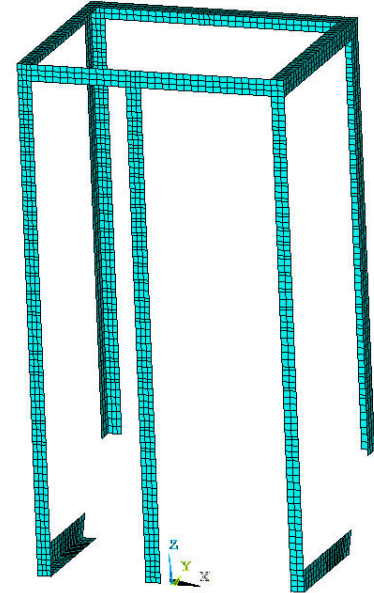
Case	Depth (mm)	Width (mm)	Length (mm)
D0	Without plaque		
D1	1	10	300
D2	2		
D3	3		
D4	4		



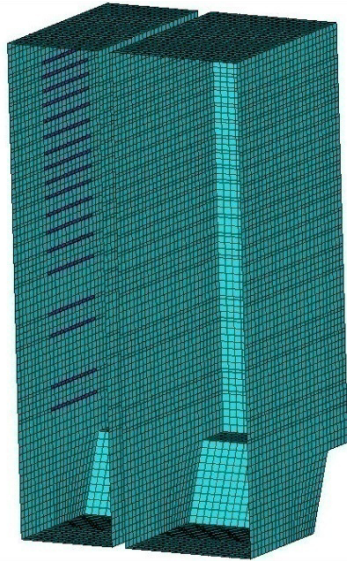
(a) PU foam



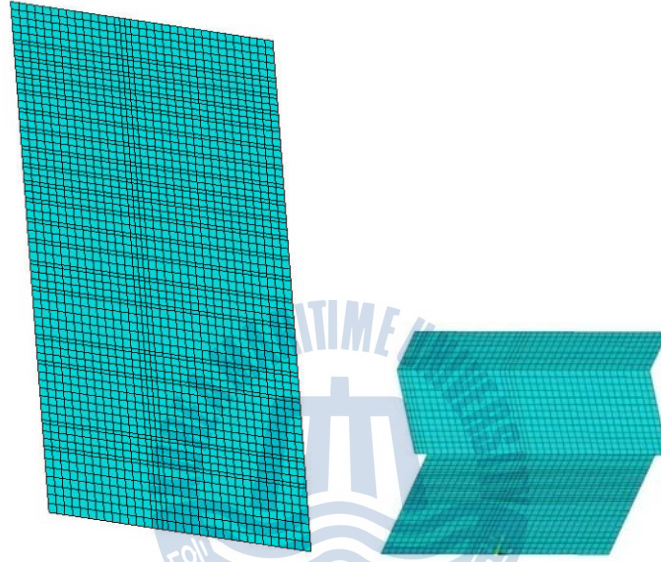
(b) Outer plate



(c) Steel frame



(d) Inner case

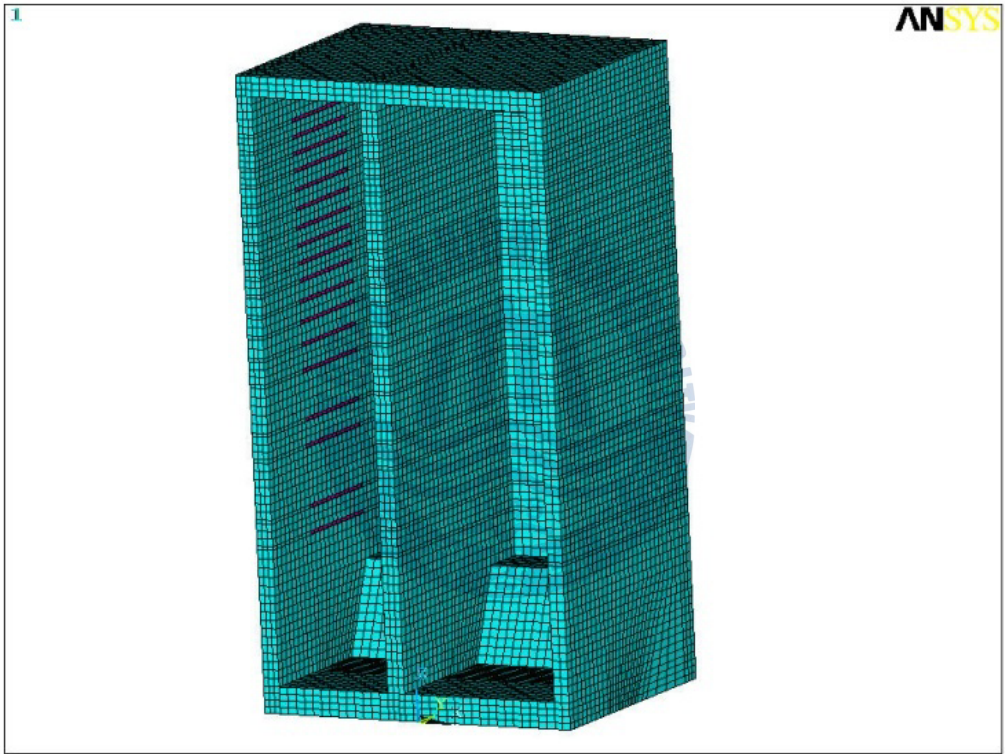


(e) Black plate

(f) Bottom plate



(g) Support plate



(h) Whole FE model

Fig. 4 FE model for cabinet

2.2.2 Mathematical Model of Steady Heat Transfer and Thermal Stress

(a) Mathematical Model of Steady Heat Transfer

In using ANSYS, it is very important to select a suitable model and set suitable boundary conditions. In this study, the assumptions were as following:

1. Temperature remains constant throughout the refrigerator;
2. Heat transfer coefficients of all components remain uniform;
3. Radiation is ignored in the heat transfer process;
4. Thermal contact resistances between all components are ignored.

Based on the previous assumptions, the heat transfer process could be treated as simple static heat conduction and convection process; the heat transfer differential equation is as following:

$$\frac{\partial}{\partial} \left(\lambda \frac{\partial T}{\partial x_i} \right) = 0 \quad (2-1)$$

λ is the uniform conduction coefficient which is obtained by experiment, W/K/sec); $i=1, 2, 3$, means the three dimension, or x, y, z.

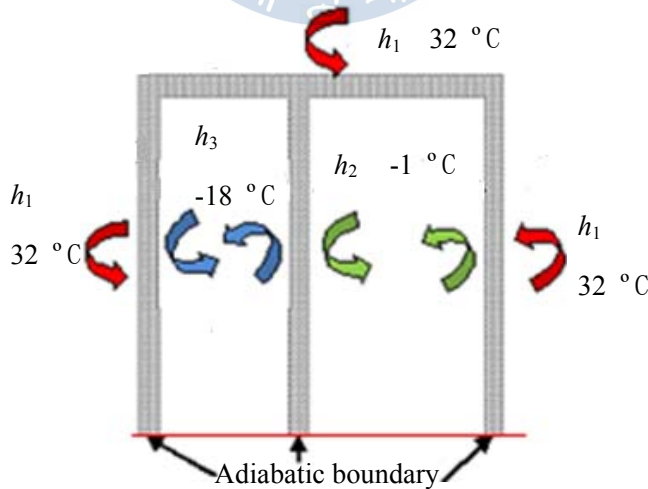


Fig . 5 Analysis condition

Analysis of thermal effect on structure components were carried out under steady state conditions. By using finite element method, static thermal analysis can ascertain such thermal parameters as temperature, thermal gradient, heat transfer flux, heat flux density and so on induced by static thermal load.

Usually, under operational condition, we assumed room temperature in summer was about 32°C, the freezer temperature and storage case are -18°C and -1°C respectively. Material properties are shown the Table-3. Heat transfer coefficients for outer space, freezer inner case and storage are respectively shown in Table 4.

Table 3 Material property

Material	Elasticity Modulus (GPa)	Poisson's Ratio	Thickness (mm)	Thermal Expansion Coefficient (1/°C)	Thermal Conductivity (W/m ² /K)
Steel(EGI)	131.7	0.31	0.6/1.2	1.17e-5	45
Steel sheet	206.8	0.29	0.3/0.4/30	1.17e-5	45
ABS_RS656H	2.11	0.38	1.5	6.9e-5	0.0206
PU Foam	3.63e-3	0	--	8e-5	0.0206

Table 4 Parameters for analysis

	Plate thermal conductivity(W/m ² /K)	Plate thickness (mm)
Steel Plate	$k_1=45$	0.6
ABS	$k_2=k_3=0.0206$	1.5

Material properties were derived from the test data provided by company. Convective heat transfer coefficients were $h_1=3\text{W/m}^2\text{k}$, $h_2=8\text{W/m}^2\text{k}$ and $h_3=22\text{W/m}^2\text{k}$ as shown in Table 5. In this study, we calculated the thermal resistance and equivalent convective heat transfer coefficient as in Table 5.

Table 5 Equivalent convective heat transfer coefficient ($\text{W/m}^2/\text{K}$)

Location	Thermal Resistance	Equivalent Convective Heat Transfer Co.
Outer Plate	$R_{out} = \frac{1}{h_1} + \frac{L}{k_1} = \frac{1}{3} + \frac{0.0005}{45} = 0.3333$	$h_{o,eq.} = 2.99990 \approx 3$
Storing Room	$R_{inner} = \frac{1}{h_2} + \frac{L}{k_2} = \frac{1}{8} + \frac{0.0015}{0.0206} = 0.1978$	$h_{s,eq.} = 5.05510 \approx 5.1$
Freezing Room	$R_{inner} = \frac{1}{h_3} + \frac{L}{k_3} = \frac{1}{22} + \frac{0.0015}{0.0206} = 0.1182$	$h_{f,eq.} = 8.45523 \approx 8.5$

(b) Mathematical Model of Thermal Stress

The refrigerator is typical model under thermal stress. Because of temperature differences between the outside environment and inside the case, stress will arise from components restraint, which is called thermal stress.

According to linear thermal elasticity theory, particles inside the body will move relatively resulting in strains, which could be superposed by the algebra method. The assumptions in thermal stress analysis are as following:

1. Heat generated due to deformation is ignored;
2. Gravity of components is ignored when making static thermal stress analysis;

So the analytical expressions of deformation compatibility equations are as following:

$$\nabla^2 \sigma_x + \frac{1}{1+\mu} \frac{\partial^2 \Theta}{\partial x^2} = -\alpha_t E \left(\frac{1}{1-\mu} \nabla^2 T + \frac{1}{1+\mu} \frac{\partial^2 T}{\partial x^2} \right) \quad (2-2)$$

$$\nabla^2 \sigma_y + \frac{1}{1+\mu} \frac{\partial^2 \Theta}{\partial y^2} = -\alpha_t E \left(\frac{1}{1-\mu} \nabla^2 T + \frac{1}{1+\mu} \frac{\partial^2 T}{\partial y^2} \right) \quad (2-3)$$

$$\nabla^2 \sigma_z + \frac{1}{1+\mu} \frac{\partial^2 \Theta}{\partial z^2} = -\alpha_t E \left(\frac{1}{1-\mu} \nabla^2 T + \frac{1}{1+\mu} \frac{\partial^2 T}{\partial z^2} \right) \quad (2-4)$$

$$\nabla^2 \tau_{xy} + \frac{1}{1+\mu} \frac{\partial^2 \Theta}{\partial x \partial y} = -\frac{\alpha_t E}{1+\mu} \frac{\partial^2 T}{\partial x \partial y} \quad (2-5)$$

$$\nabla^2 \tau_{yz} + \frac{1}{1+\mu} \frac{\partial^2 \Theta}{\partial y \partial z} = -\frac{\alpha_t E}{1+\mu} \frac{\partial^2 T}{\partial y \partial z} \quad (2-6)$$

$$\nabla^2 \tau_{zx} + \frac{1}{1+\mu} \frac{\partial^2 \Theta}{\partial z \partial x} = -\frac{\alpha_t E}{1+\mu} \frac{\partial^2 T}{\partial z \partial x} \quad (2-7)$$

Θ – Volume force, and $\Theta = \sigma_x + \sigma_y + \sigma_z$

$\sigma_x, \sigma_y, \sigma_z$ -stresses along x,y,z axis;

$\tau_{xy}, \tau_{yz}, \tau_{zx}$ - shearing stresses;

E -elasticity modulus;

μ -Poisson' ratio;

α_t - Linear expansion coefficient.

The boundary conditions are set so that the bottom points of the refrigerator are fixed.

As we all know, the behavior of structures when subjected to thermal effect is

$$\varepsilon_{total} = \varepsilon_{thermal} + \varepsilon_{mechanical} \quad (2-8)$$

With $\varepsilon_{mechanical} \rightarrow \sigma$ and $\varepsilon_{total} \rightarrow \delta$

The total strains govern the deformed shape of the structure δ through kinematic or compatibility considerations^[12]. By contrast, the stress state in the structure σ (elastic or

plastic) depends only on the mechanical strains. Where the thermal strains are free to develop in an unrestricted manner, there are no external loads, axial expansion or thermal bowing results from

$$\varepsilon_{total} \rightarrow \varepsilon_{thermal} \quad \text{and} \quad \varepsilon_{total} \rightarrow \delta$$

By contrast, where the thermal strains are fully restrained without external loads, thermal stresses and plastification result from

$$0 = \varepsilon_{thermal} + \varepsilon_{mechanical} \quad \text{with} \quad \varepsilon_{mechanical} \rightarrow \sigma$$

The single most important factor that determines a real structural response to thermal change is the manner in which it responds to the unavoidable thermal strains induced in its members through thermal change.



2.3 Structural Analysis Process

Assume that the environment temperature is 32°C , and temperatures in freezer room and storage room are -18°C and -1°C respectively. An *.rth file of thermal analysis result would be stored and called for use in the next structural analysis process. The analysis process is composed by three steps:

- Pre-process: modeling;
- Solution: loading and calculating;
- General post process: check up the results

The thermal analysis process is shown as in Fig.6. A named sequential thermal-mechanical coupling analysis method was used in this study. The structural analysis model was based on the thermal modeling, which was already constructed in the preceding thermal analysis process. The first step for us to do was to remove all the thermal loading and change thermal element to structural element.

Then we had to set the other material properties including elasticity, Poisson's ratio, and the thermal expansion coefficient. The steel plate and ABS inner liner would be constructed by re-meshing the solid face according to different material properties, real constants and element types. The flow chart for this is as shown in Fig. 7.

As for the load condition, we need the temperature load and to fix the four points at the corner in the bottom face after constructing support plate. The temperature load is inputted by a 'rth' file generated in the thermal analysis process. In order to fix the four points with APDL, we have to know the point numbers. It's easily to realize such a tentative idea using *get method with APDL. The following is given to show how to identify the point numbers and fix them.

Firstly, we changed the solid element of the PU foam part to structural analysis

element of solid-185. We assigned real constants of the shell elements for every sheet part. Next, we re-meshed the sheet areas with different thickness and material properties. Then, called for the *.rst file which was obtained in the previous thermal analysis process.

Under nominal conditions, the cabinet sits on four rollers. So the four points on the bottom were fixed as boundary conditions in the actual environment.

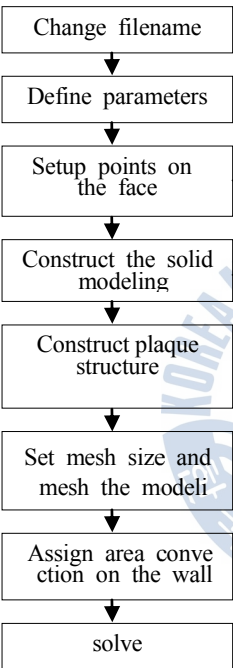


Fig. 6 Flow chart of thermal analysis

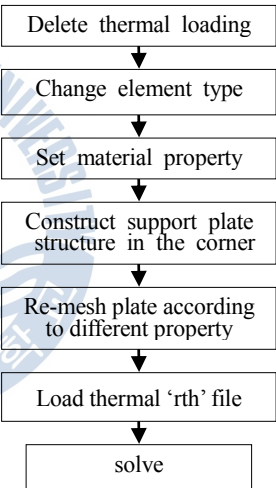


Fig. 7 Flow chart of structural analysis

2.4 Analysis Results and Discussion

2.4.1 Analysis Results

The analysis results are shown in the following Fig. 8~15 and Table 6.

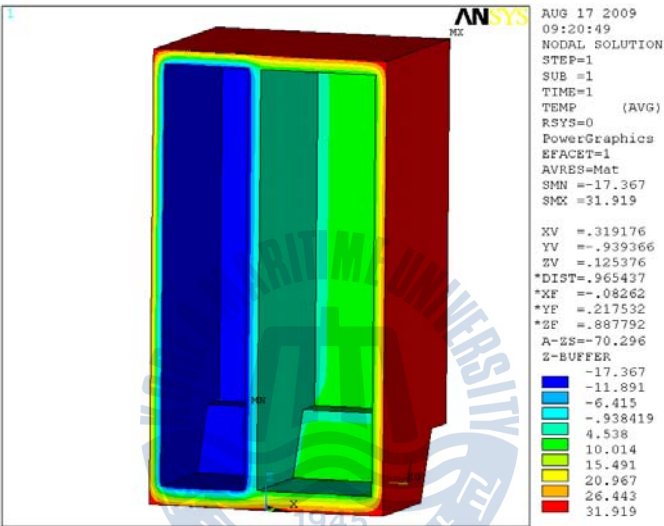


Fig. 8 Temperature distribution of model-D0

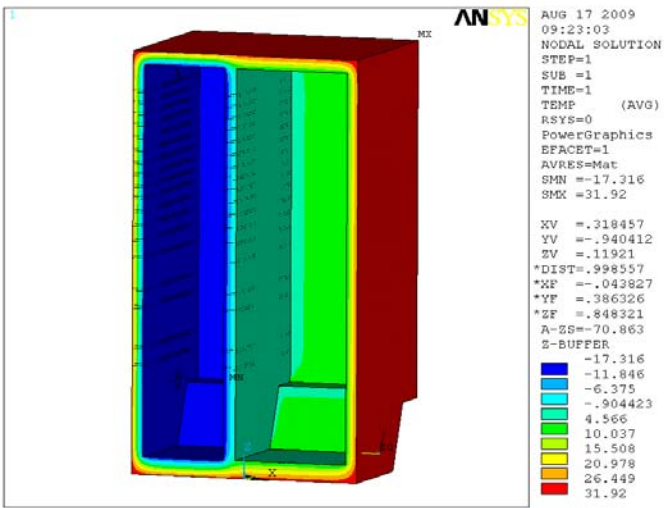


Fig. 9 Temperature distribution of model-D1

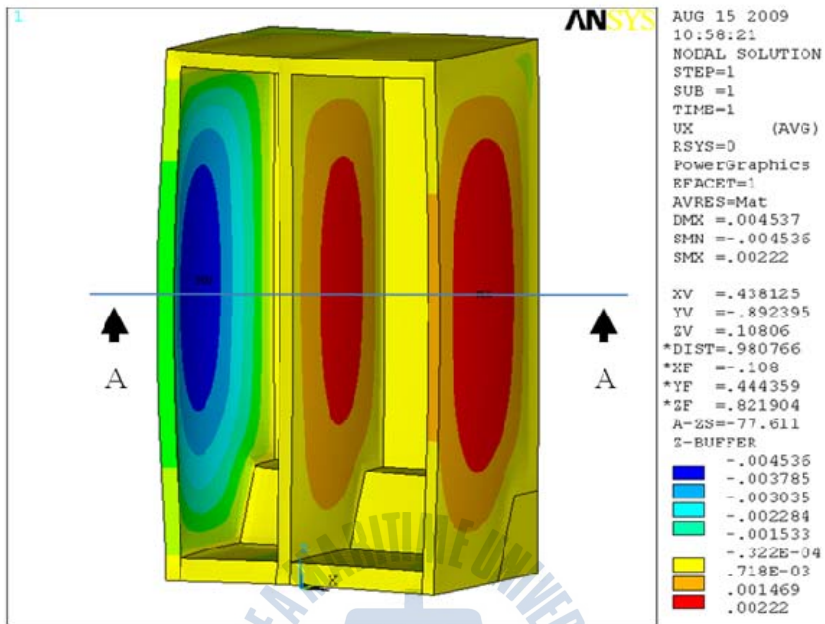


Fig. 10 X-displacement of model-D0

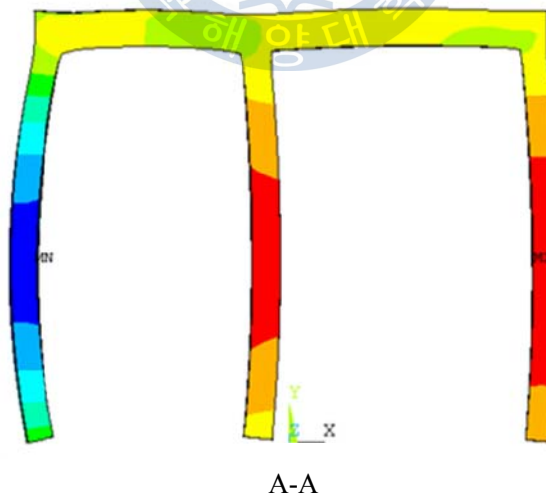


Fig. 11 X-displacement at middle cross section

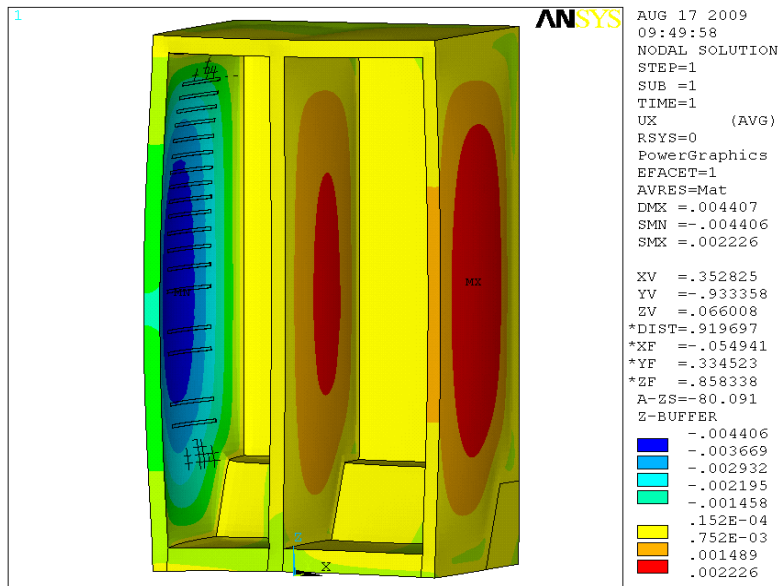


Fig. 12 X-displacement of model-D1

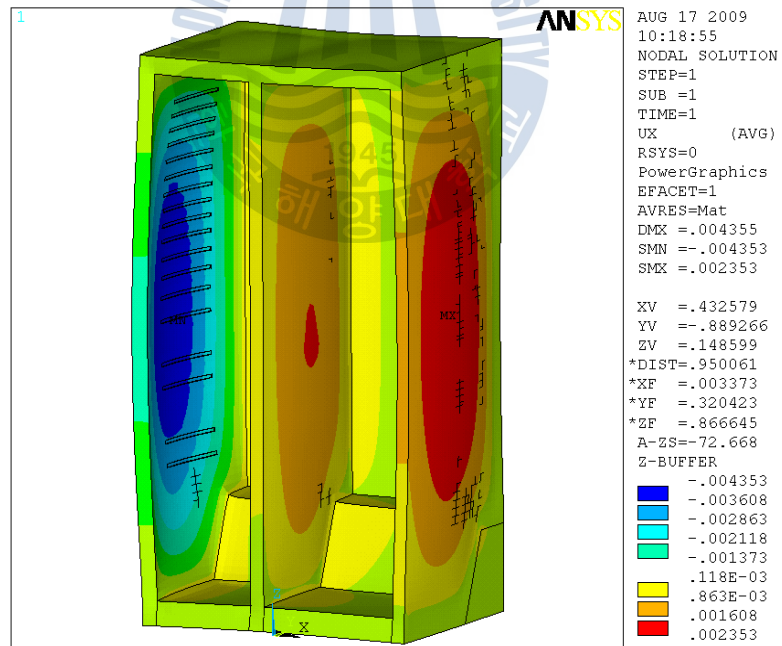


Fig. 13 X-displacement of model-D2

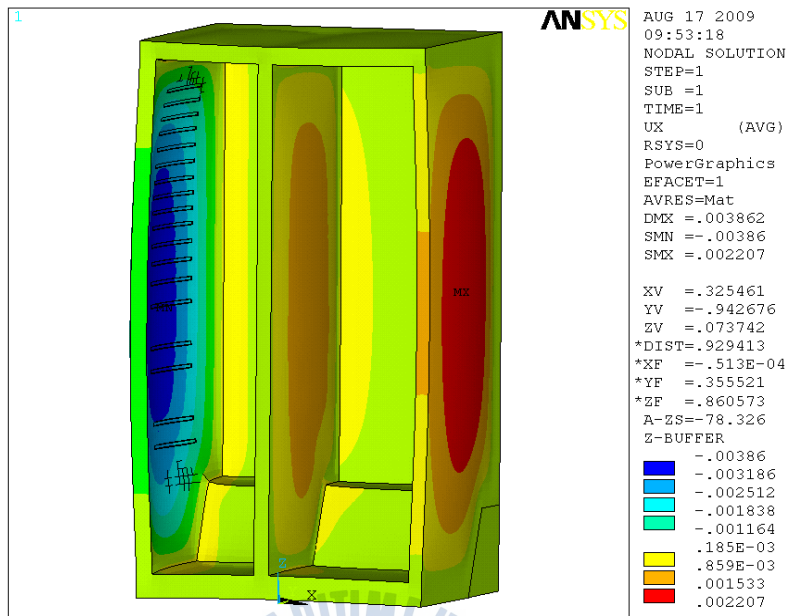


Fig. 14 X-displacement of model-D3

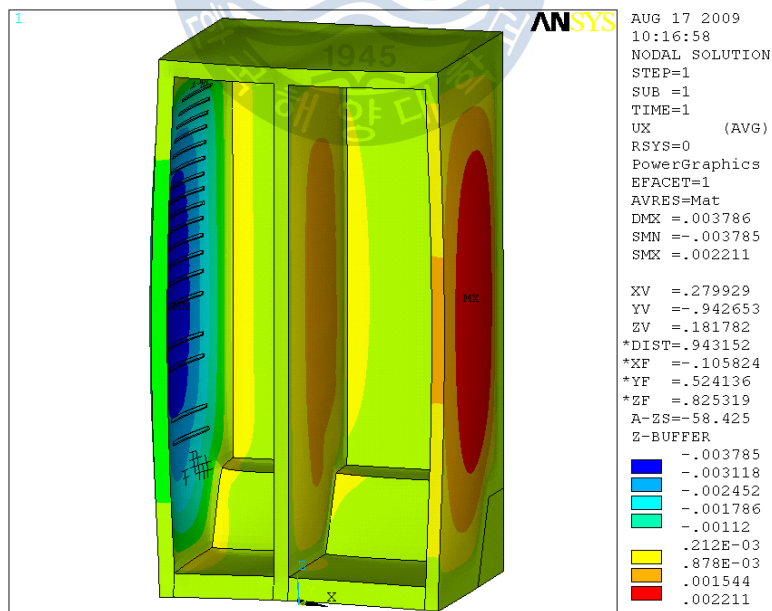


Fig. 15 X-displacement of model-D4

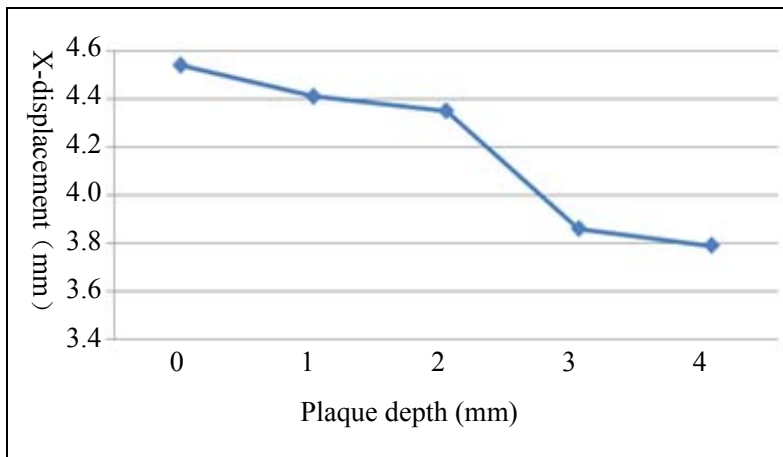


Fig. 16 Comparison of structural analysis results

Table 6 Structural analysis results

Model	D0	D1	D2	D3	D4
Deformation(mm)	4.54	4.41	4.35	3.86	3.79

2.4.2 Discussion

The behavior of the refrigerator when subjected to thermal effect was found to have two different deformations.

- (1) Thermal deformation under uniform temperature condition.

The outside steel plates were exposed to the environment and the inner ABS inner compartment endured uniform temperature condition throughout the whole refrigerator. ABS inner compartment would contract uniformly according to actual constraint condition with negative temperature.

Uniform temperature induces thermal expansion (or contraction if under decreasing

temperature condition) strains ε_T , in most structural materials. These are given by

$$\varepsilon_T = \alpha \cdot \Delta T \quad (2-9)$$

The PU foam material has a larger coefficient of linear expansion than the ABS material, which would cause much more contraction inducing tensile stress on ABS inner case. This would cause the ABS layer to crack under extreme test or operating condition.

(2) Thermal deformation under normal operating condition

A thermal gradient would exist throughout the PU foam compartment in the thickness direction. However, this causes the inner part of PU foam to contract while the outer part expands inducing bending in the component. This effect is called thermal bowing and is the main deformation that dominates the magnitude of the refrigerator inner case deformation under extreme operating conditions.

Test results confirm that the plaques are effective as expansion joints to relieve liner surface tension. Some studies showed that the unplaqued samples exhibited yield forces which averaged 146,000psi at 1% tensile deflection. The plaqued samples exhibited yield forces, which averaged 32,000psi at 1% tensile deflection. Because the plaqued liner samples have only 22% of the internal stiffness of the flat unplaqued liner samples, the plaqued material is more resistant to cabinet bowing. So, many refrigerator inner cases have been designed as plaqued shape ^[13].

Results show that plaques are helpful to reduce thermal bowing deformation in the refrigerator sidewall. It is probably because plaques increase the surface area and increase structural rigidity of the inner case. The maximum thermal bowing deformation always occurs on the sidewall between the freezer and the outside. It can be seen in Fig.16 that the deeper the plaque is; the more obvious is the effect of decreasing of thermal deformation.

Chapter 3 Structural Optimization of refrigerator

3.1 Introduction

Mathematical programming techniques are used to find the minimum of a function of several variables under a prescribed set of constraints, such as: calculus methods, nonlinear programming, geometric programming, quadratic programming, and sequential quadratic programming (SQP), linear programming, genetic algorithm (GA) etc. The choice of methods depends on the type of problems being solved. There is no single method to solve all optimization problems efficiently. Hence we should try various methods in order to choose the best one that proves to be computationally efficient and accurate. The subsequent subsections of this topic provides a brief discussion on the optimization methods used in this research work along with a discussion of the optimality criterion known as “Sub Problem” employed in the ANSYS Classic to find the optimal solution to a design problem. GA differs from more traditional optimization techniques in that it involves a search from a “population” of solutions, not from single points. Each iteration or generation of a GA involves a competitive selection that weeds out poor solutions. The solutions with high “fitness” are “recombined” with other solutions by swapping parts of solutions with another.

In this chapter, we separately used FEM and GA to take structural optimization of refrigerator. We utilized an Artificial Neural Network (ANN) to set up a nonlinear mapping relation between parameters of plaque with thermal deformation. We presented a new idea to take an accurate optimization analysis of complex structure, especially in the event that we don't have sufficient experiment data.

3.2 Parametric Modeling

APDL is a scripting language that has been used here to build the model and automate tasks by using parameters (variables). An extensive APDL file was used to create the model with plaques. A sequence of ANSYS commands can be recorded in a macro file which enables us to create a customized ANSYS command that executes all of the commands required for a particular analysis. APDL is the foundation for sophisticated features such as design optimization and adaptive meshing. In order to make a parametric refrigerator model, the whole model was divided into several parts according to the characteristic dimensions as shown in the following Fig. 17~18.

The APDL file control program sets up reference points which outline every part of the refrigerator model. The first step is to setup the points to make an original solid modeling of PU foam, which is in an early form of complete refrigerator modeling. To make such a model, we need geometric parameters, including length, height, width of the freezer inner case and the storage case outline, and refrigerator wall thickness. Moreover, we need material parameters because PU foam material properties are changed under different temperatures or when using different test methods. Therefore, we need to change the material properties later by modifying the parameters in visual interface. Then we need to add the plaque parameters into the refrigerator modeling, including amount, length, width, depth, and distance between the plaques. We have to divide the whole refrigerator model into parts according to the plaques. In addition, it is very important to remember the position of every plaque face so that we are able to change the parametric depth. APDL provides with us several convenient program flow control methods including `*do-*endo`, `*if-*ifelse-*else-*endif`, `*repeat`. After executing the codes if we input data for parameters, the model would be setup automatically as in Fig. 19. Table 7 and Table 8 listed the

parameters of cabinet and plaque.

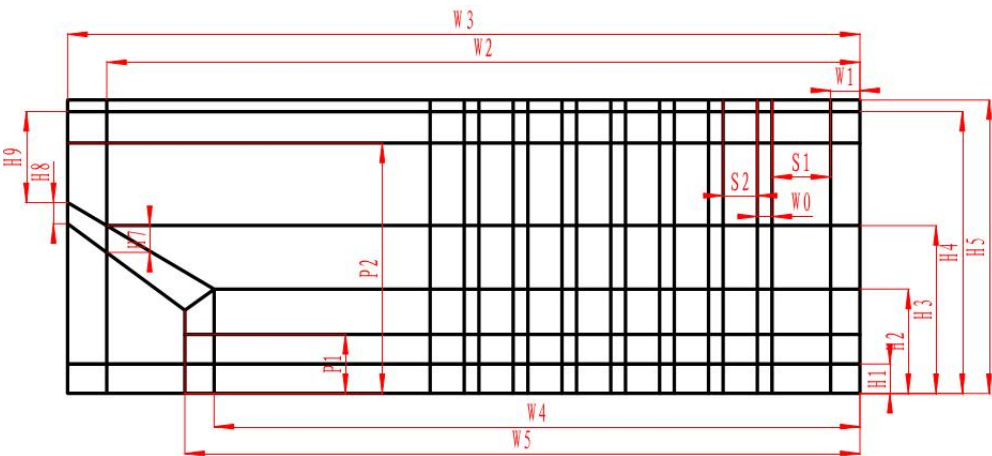


Fig. 17 Parameters on side view

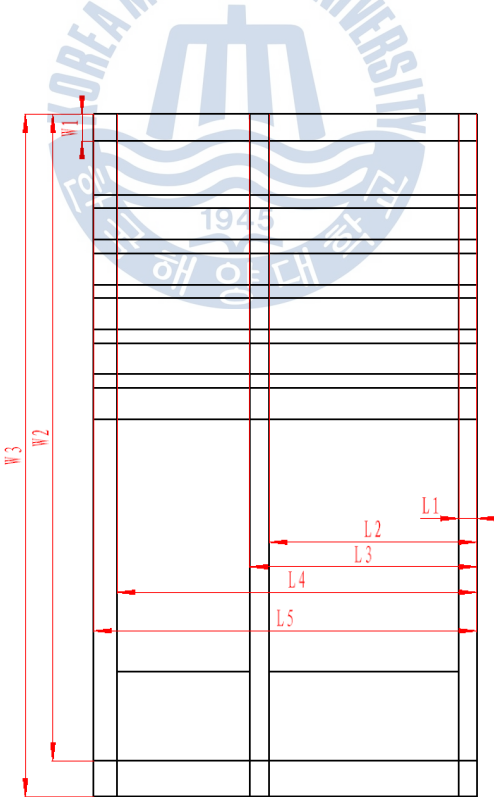
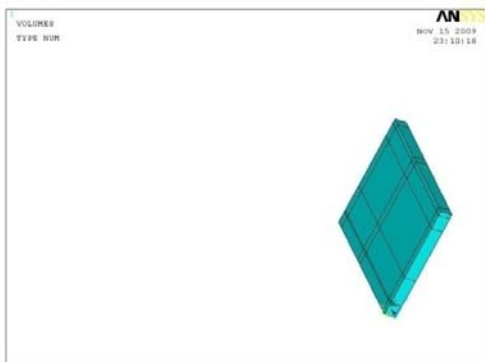
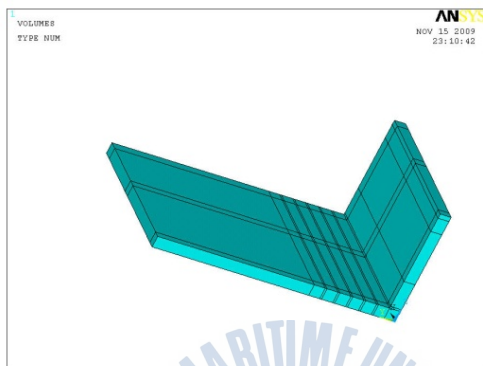


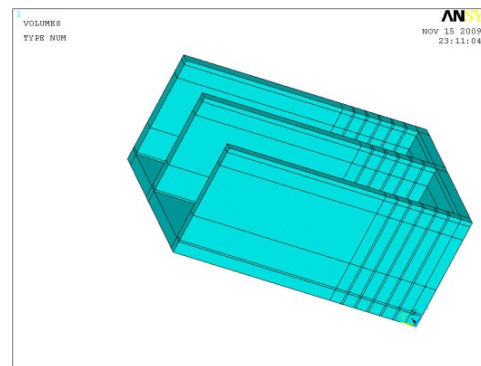
Fig. 18 Parameters on front view



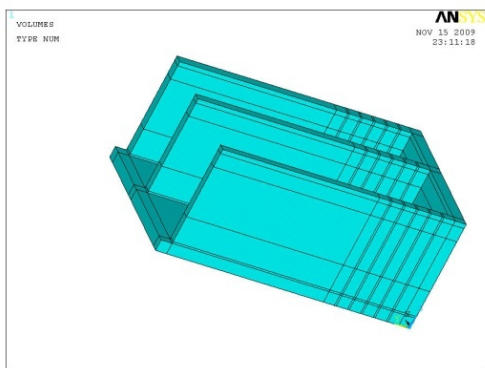
(a)



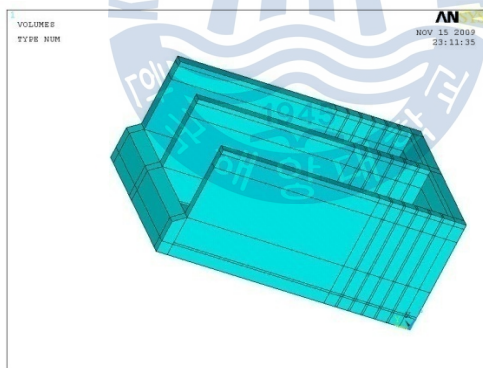
(b)



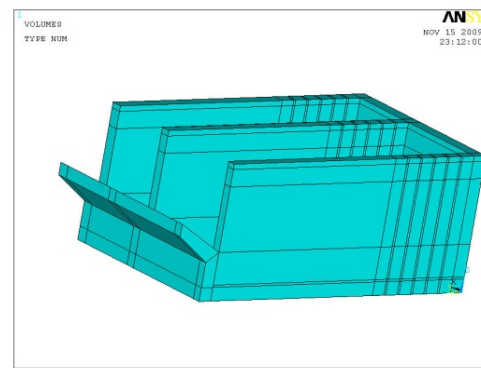
(c)



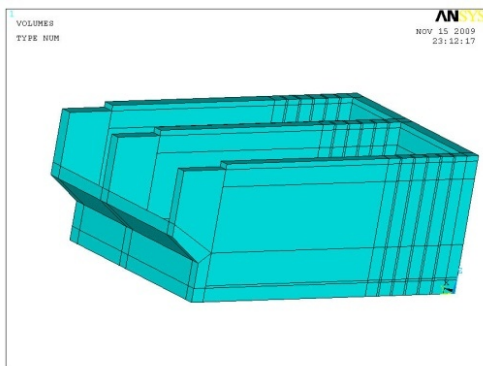
(d)



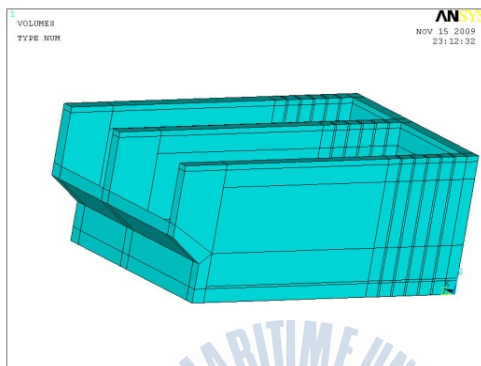
(e)



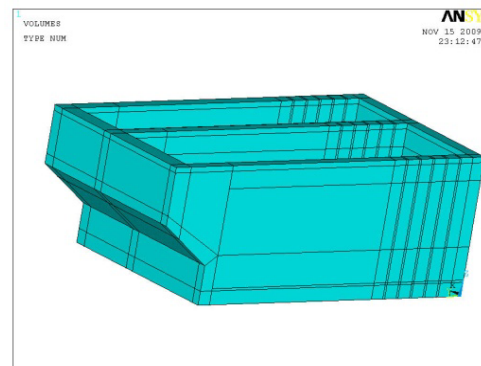
(f)



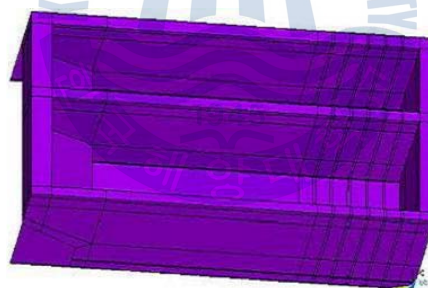
(g)



(h)



(i)



(j)

Fig. 19 Parametric modeling process

Table 7 Geometry parameters of refrigerator model

Height	Width	Length	Positioning parameters
H1	W1	L1	P1
H2	W2	L2	P2
H3	W3	L3	S1
H4	W4	L4	S2
H5	W5	L5	
H6			
H7			
H8			
H9			

Table 8 Plaque parameters

Plaque Parameters	Unit: mm
Depth	1~3
Width	10~20
Interval Distance	10~125
Numbers	6~18

The primary factor to make a refrigerator model with plaques is that there are numbers of identical plaques on the wall. We only have to construct a cycling process to automatically setup similar plaque structure at regular intervals in the refrigerator height direction. The modeling flow chart is given as in Fig.20.

We have to be aware that our purpose is to identify the plaque effect on the wall deformation and the plaque's geometric parameter would be frequently changed later. Therefore, in the modeling process, we have to pay attention to the plaque's height because the refrigerator modeling has been divided into many parts, and if it is so happened that, the plaque points are located on the partition position, errors would certainly arise because no solid would be constructed. Our method is to use a lot of *if-*else if-*then-*end if.

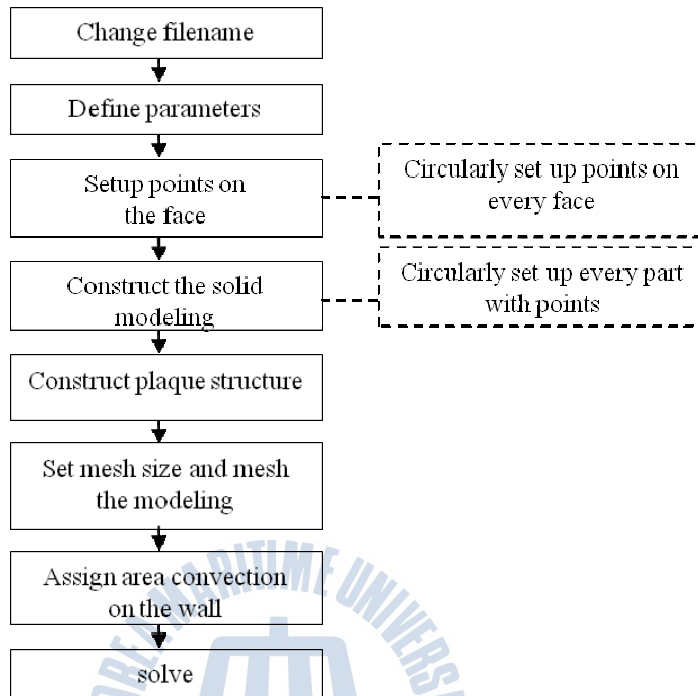


Fig. 20 Flow chart of parametric modeling

The outer plate material is steel, the inner case is ABS_RS656H plastic; a layer of foam is inserted between the steel and the plastic liner which acts as thermal insulation and provides structural rigidity to the refrigerator cabinet.

3.3 Structural Optimization Using FEM

The structural optimization is necessary to be applied to the refrigerator inner case according to the earlier analysis in chapter 2. Structural optimization has been and continues to be a large area of active research. Vanderplaats^[14] appeared to be among the few whom were successful in applying numerical approaches such as gradient method, sequential quadratic programming, and approximation methods to the optimization of structures. Many of these techniques were based on the Taylor series expansion of the objective and the constraint function with respect to the design variables. Typically, the Taylor series expansion is used to linearize a non-linear system in order to apply operations research techniques. It is important to note that it is these same numerical methods that are present in some FEA software such as ANSYS^[15]. Apart from Vanderplaats, Salajegheh et al.^[16] and Hansen et al.^[17] also followed a similar approach using an approximation method based on first order Taylor series expansion of the member forces. In addition, Smith and Miura^[18] also used an approximate technique based on Taylor series expansion for the sizing problems. Imai^[19] used numerical methods based on Lagrange multipliers often referred to as the primal–dual method. This method is capable of handling both equality and inequality constraints.

Application of linear programming techniques to structural optimization was also heavily studied by Belegundu^[20], Qian et al.^[21], Hall et al.^[22], Erbutur and Al-Hussainy^[23], just to name a few. To date, no single mathematical method has been found to be entirely efficient and robust for the entire range of engineering optimization problems.

Apart from the above Mathematical Programming (MP) based approaches, optimality criterion methods that utilize the Kuhn–Tucker condition with Lagrangian multiplier was also used for structural optimization by Gellatly and Berke^[24], Venkayya et al.^[25], Allwood and Chung^[26], Kirsch^[27], Chang^[28], Rozvany and Zhou^[29], just to name a few. In structural

optimization it is well known that Optimality Criteria (OC) techniques and MP based methods have received great interest and application during the last several decades^[30].

Several methods and tools are offered in ANSYS that in various ways attempt to address the mathematical problems. One of these is the sub-problem approximation method of optimization that can be described as an advanced, zero-order method in that it requires only the values of the dependent variables (the objective function and state variables) and not their derivatives. The dependent variables are first replaced with approximations by means of least squares fitting, and the constrained minimization problem is converted to an unconstrained problem using penalty functions. Minimization is then performed every iteration on the approximated, penalized function (called the sub problem) until convergence is achieved or termination is indicated.

3.3.1 Structural Optimization of refrigerator using FEM

The plaques were designed within designated distance of 740mm. We should firstly make certain about effect of variables of plaque depth, width and numbers on refrigerator thermal deformation. Then, with designated numbers, we analyzed the effect of plaque depth, width and interval distance between plaques on refrigerator thermal deformation.

We designed optimization analysis file to set up parametric FE refrigerator model by using APDL of ANSYS software. The analysis process is designed as the following Fig.21

The key factor is to set up mathematics model for structural optimization analysis in actual mechanical optimal design. We should set the optimal object, select design variables and state variables to set up object functions and set constraint conditions.

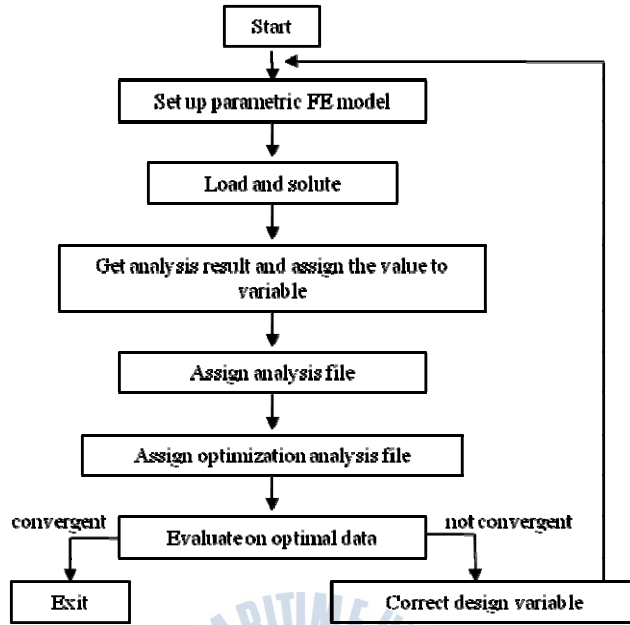


Fig. 21 Optimization analysis process

(a) Objective Function

In this studying, the internal stresses for each material are in low level that would not exceed the fracture strength. We concern more with thermal deformation for the refrigerator with plaques. We want to obtain the minimum thermal deformation by optimal plaques parameters. However, thermal deformation has so complicated relations with plaque parameters that we could not express them in explicit functions. The objective function is descriptive in implicit function as following:

$$T.D. = f(X_1, X_2, X_3, X_4) = f(D, W, S, N) \rightarrow \min \quad (3-1)$$

D -plaque depth;

W -plaque width;

S -interval distance between plaques;

N -Plaque numbers;

$T.D.$ -Thermal deformation of inner case

In this studying, the program would give out a functional curved surface for the object function and design variables by optimal cycling calculation^[15]. Usually in the next iteration step, new generated data would fit and renew the functional curved surface of the previous step.

For this project, assuming that equation-1 has continuous differentiability within value range of design variables. The iteration method would generate a serious of design variables points $\{D_k, W_k, S_k, N_k\}$, and object function value would descend in the next iteration step.

$$f(D_{k+1}, W_{k+1}, S_{k+1}, N_{k+1}) - f(D_k, W_k, S_k, N_k) < 0 \quad (3-2)$$

The design variable vector should be determined in every iteration step.

$$x^{j+1} = x^j + c(\tilde{x}^j - x^b) \quad (3-3)$$

\tilde{x}^j — the design variable vector corresponding to unconstrained objective function

x^b — Best design set constants

c — Internally chosen to vary between 0.0 and 1.0, based on the number of infeasible solutions.

Convergence is assumed when either the present designed set, x^j , or the previous design set, x^{j-1} , or the best design set, x^b , is feasible; and one of the following conditions is satisfied.

- 1) objective function difference between best design set and the present design set should be less than objective function tolerance

$$|f^j - f^b| \leq \tau \quad (3-4)$$

- 2) difference between two design sets should be less than objective function tolerance

$$|f^j - f^{j-1}| \leq \tau \quad (3-5)$$

- 3) differences between best design set and all design sets should be less than their tolerance

$$|x_i^j - x_i^b| \leq \rho_i (i=1,2,\dots,n) \quad (3-6)$$

4) differences between two design sets should be less than their tolerance

$$|x_i^j - x_i^b| \leq \rho_i (i=1,2,\dots,n) \quad (3-7)$$

τ and ρ_i —objective function and design variable tolerances

(b) Design Variables

Design variables are those factors that would directly affect design quality and analysis results. The more design variables were selected, the more complicated the analysis problem would be. For the refrigerator with plaques, the parameters of plaque depth, plaque width, plaque numbers and interval distance between plaques are considered to have more obvious effect on refrigerator thermal deformation than other parameters. Vectorial design variable descriptions are as the following:

$$X=[X_1, X_2, X_3, X_4]^T=[D, W, S, N]^T \quad (3-8)$$

In the first analysis, the distance of the area with plaques is 740mm on the refrigerator wall. Then the interval distance between plaques would be calculated by the following equation:

$$S = (740 - W \times N)/(N - 1) \quad (3-9)$$

Even numbers as 6, 8, 10, 12, 14, 16, and 18 are chosen to make the optimization models. According to the actual refrigerator structure, the value range of design variables is set by (unit: mm):

$$1 \leq D \leq 3$$

$$10 \leq W \leq 30$$

$$N=6,8,10,12,14,16,18$$

The interval distances between plaques are set to be within the following values so that plaques would be properly arranged along the inner liner in the parametric model, as shown in Table 9.

Table 9 Interval distance with different plaque numbers

Plaque number (N)	6	8	10	12	14	16	18
Interval distance <i>S</i> (mm)	10~136	10~94	10~71	10~56	10~46	10~38	10~32

For the discrete design variable problem, usually we utilize control flow statement (as *if-then-*else, or *do statement, or nint()-round number) by APDL to control optimization program. When plaque numbers are designated to constants, design variables are set to be plaque depth, width, and interval distance between plaques.

(c) State Variable

State variables are those parameters that set constraint conditions for and have some functional relations with design variables. In the first analysis, we did not select any functional state variables so that it is simplified to an unconstrained problem. When plaque numbers are designated to constants, select total distance of plaque area as state variable. The total distance of plaque area was calculated by the following equation:

$$T.S. = W \times N + S \times (N - 1) \quad (3-10)$$

$$110 \leq T.S. \leq 740$$

T.S. was treated as a state variable in this optimization analysis.

3.3.2 Optimization Analysis Results (Design variables: *D*, *W* and *N*)

Firstly, we tried to find out how many plaques are the most suitable in the designated distance with variables of plaque depth and width to decrease thermal deformation. We set

plaque depth, width and numbers as design variables.

After ten iteration steps, program stopped when the result satisfied with the convergence condition. The optimization analysis results are listed in Table 10. The iteration processes are shown in Fig. 22~24.

Table 10 Optimization analysis result (N is variable)

Unit: mm

Iterate Number	1	2	3	4	5
Plaque Number	6	16	14	16	8
Depth	3	1.914	2.075	1.007	2.586
Width	20	17.76	22.358	19.382	21.643
DMAX	2.143	2.028	1.997	2.584	2.092
Iterate Number	6	7	8	9	10
Plaque Number	6	16	16	16	16
Depth	2.06	1.286	2.761	2.826	2.95
Width	28.176	21.28	21.544	21.063	20.568
DMAX	2.509	2.355	1.784	1.775	1.758

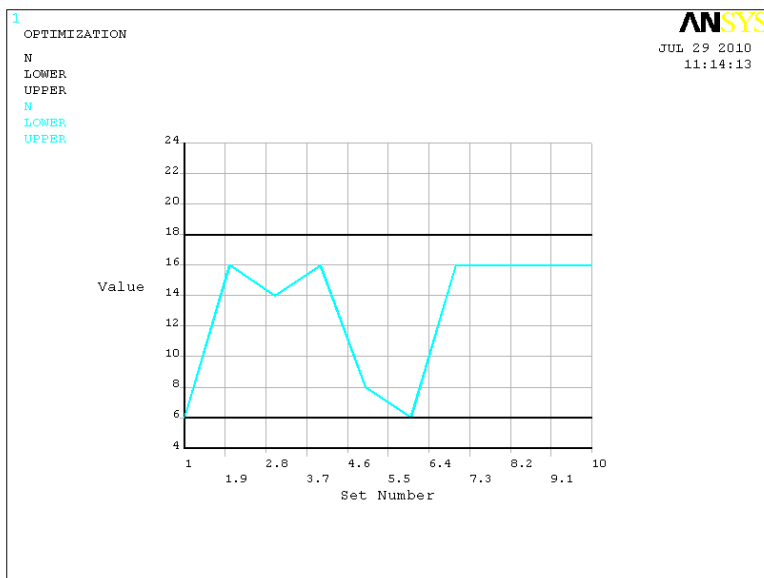


Fig. 22 Iteration process of N

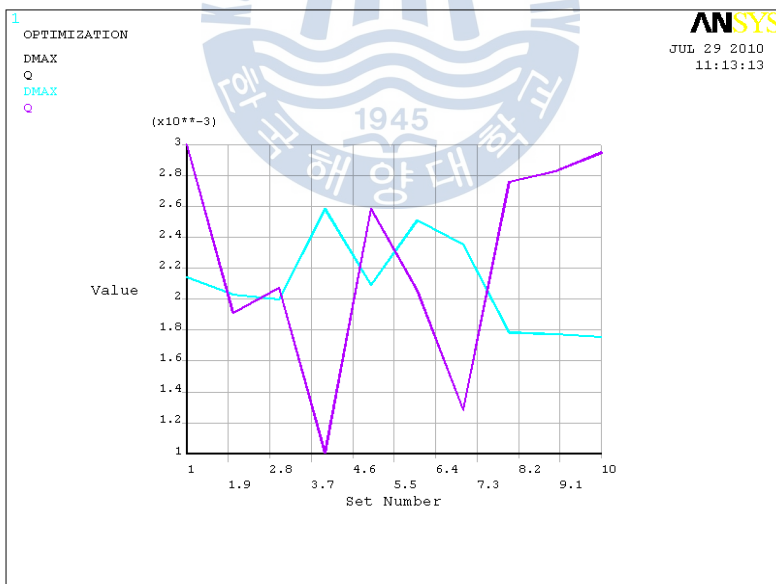


Fig. 23 Iteration process of Q and $DMAX$

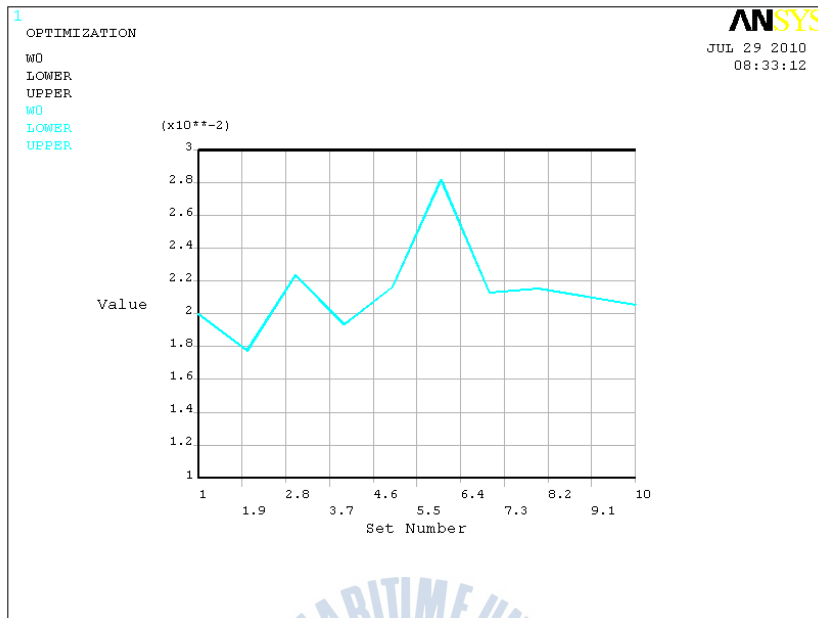


Fig. 24 Iteration process of W

From the analysis results, we can see that optimization analysis result was convergent at the last iteration number-ten. Plaque number is sixteen, depth almost approaches the upper limit 3mm, and width is about 20mm.

However, it is not good for the refrigerator thermal deformation if the plaque numbers increase continually. It is because that, the more there are plaques, the thinner is the refrigerator inner case wall.

3.3.3 Optimization Analysis Results (Design variables: D , W and S)

We separately set plaque number as 6, 8, 10, 12, 14, 16 and 18 within 740mm distance. Design variables were set as plaque depth, width and interval distance between plaques.

The optimization results are listed in the following Table 11~17 and Fig. 25~38.

Table 11 Analysis result (N=6)

unit:mm

Iteration Number	1	2	3	4	5	6
<i>T.S.</i>	160	651.33	597.64	661.41	398.01	522.96
Interval Distance	20	108.95	92.699	109.02	53.63	79.879
Depth	1	1.914	2.075	1.007	2.586	1.225
Width	10	17.76	22.358	19.382	21.643	20.595
DMAX	2.899	2.458	2.313	2.902	2.338	2.715
Iteration Number	7	8	9	10	11	12
<i>T.S.</i>	437.5	596.12	556.92	446.01	613.56	706.61
Interval Distance	56.972	87.149	85.205	74.297	96.206	114.81
Depth	20.631	2.768	2.838	2.959	2.951	2.984
Width	2.544	26.729	21.816	12.421	22.089	22.093
DMAX	2.438	2.203	2.159	2.272	2.106	2.105

Table 12 Analysis result (N=8)

unit:mm

Iteration Number	1	2	3	4	5	6
<i>T.S.</i>	290	548.55	428.6	593.54	625.45	630.75
Interval Distance	30	536.3	29.219	69.353	69.003	68.589
Depth	1	2.586	2.911	2.892	2.974	2.991
Width	10	21.643	28.008	13.509	17.803	18.828
DMAX	2.829	2.139	2.297	2.073	2.013	2.003

Table 13 Analysis result (N=10)

unit:mm

Iteration Number	1	2	3	4	5	6	7
<i>T.S.</i>	280	725.07	687.46	479.38	725.5	729.9	735.69
Interval Distance	20	60.83	51.542	29.217	55.764	50.335	55.996
Depth	1	1.914	2.075	2.586	2.805	2.943	2.929
Width	10	17.76	22.358	21.643	22.362	27.688	23.172
DMAX	2.771	2.226	2.1	2.216	1.895	1.938	1.871

Table 14 Analysis result (N=12)

unit:mm

Iteration Number	1	2	3	4	5
<i>T.S.</i>	340	545.87	687.34	728.5	73.663
Interval Distance	20	26.014	38.873	42.611	43.346
Depth	1	2.586	2.911	2.974	2.991
Width	10	21.643	21.645	21.649	21.652
DMAX	2.712	2.122	1.873	1.809	1.812

Table 15 Analysis result (N=14)

unit:mm

IterationNumber	1	2	3	4	5	6
<i>T.S.</i>	400	641.18	713.03	733.93	597.33	739.3
Interval Distance	20	26.014	31.539	33.144	16.165	36.206
Depth	1	2.586	2.911	2.974	2.991	2.991
Width	10	21.643	21.644	21.647	27.656	19.188
DMAX	2.653	1.979	1.825	1.786	2.032	1.778

Table 16 Analysis result (N=16)

unit:mm

Iteration Number	1	2	3	4	5	6
<i>T.S.</i>	460	688.45	727.54	642.85	552.14	736.47
Interval distance	20	22.812	22.804	12.771	13.429	23.398
Depth	1	2.586	2.911	2.936	2.978	2.975
Width	10	21.643	24.092	28.206	21.92	24.094
DMAX	2.601	1.872	1.772	1.982	2.058	1.75

Table 17 Analysis result (N=18)

Iteration Number	1	2	3	4	5	6	7
<i>T.S.</i>	520	451.9	513.54	663.4	719.6	603.47	736.84
Interval distance	20	12.754	10.646	23.862	26.365	14.7	25.355
Depth	1	2.583	1.403	2.907	2.974	2.991	2.604
Width	10	13.06	18.475	14.312	15.078	19.642	16.99
DMAX	2.549	2.221	2.384	1.865	1.798	1.968	1.821

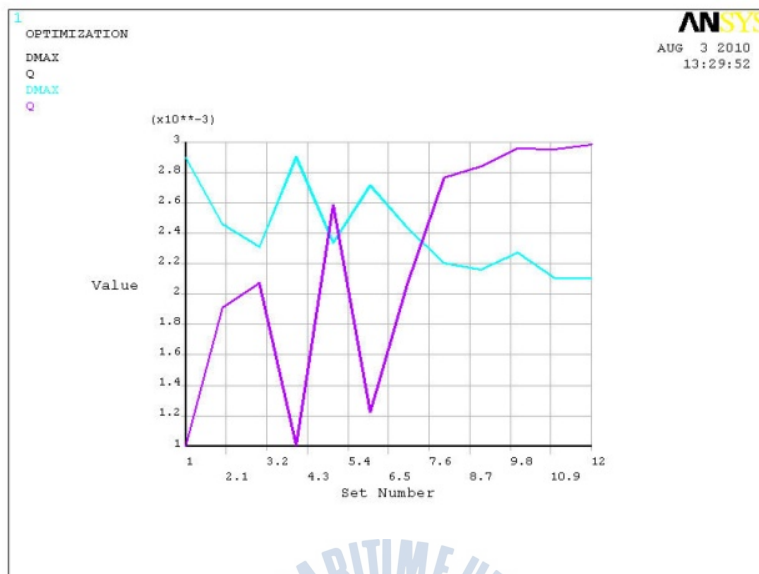


Fig. 25 Iteration process of Q and $DMAX$ ($N=6$)

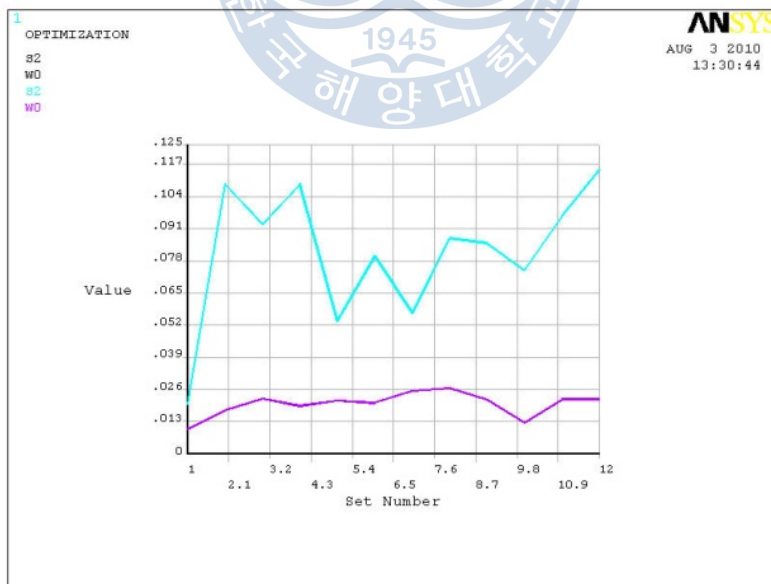


Fig. 26 Iteration process of W and S ($N=6$)

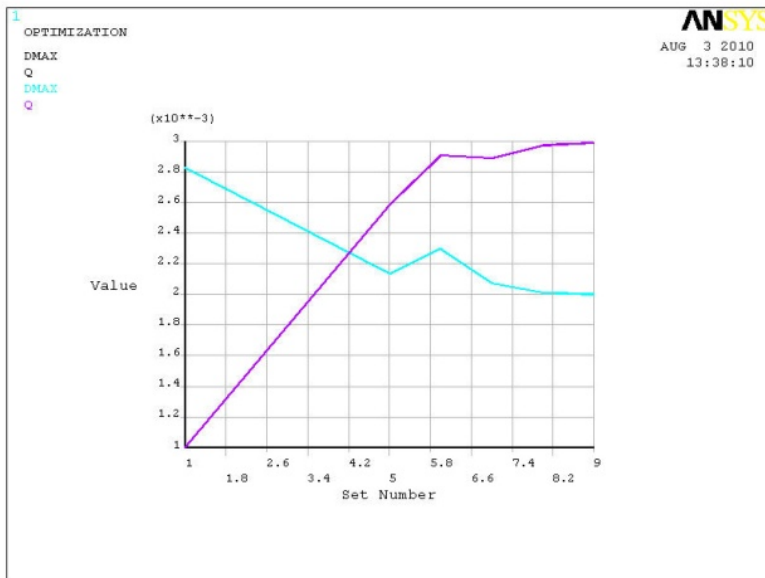


Fig. 27 Iteration process of Q and $DMAX$ (N=8)

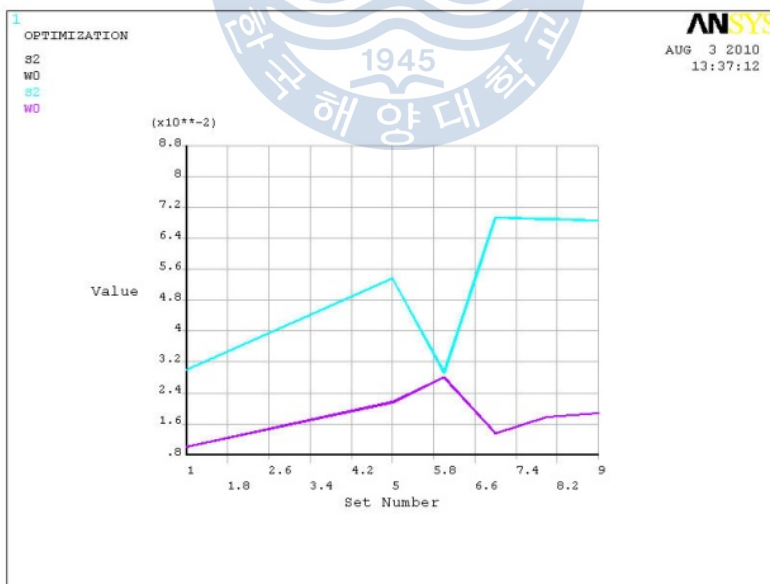


Fig. 28 Iteration process of W and S (N=8)

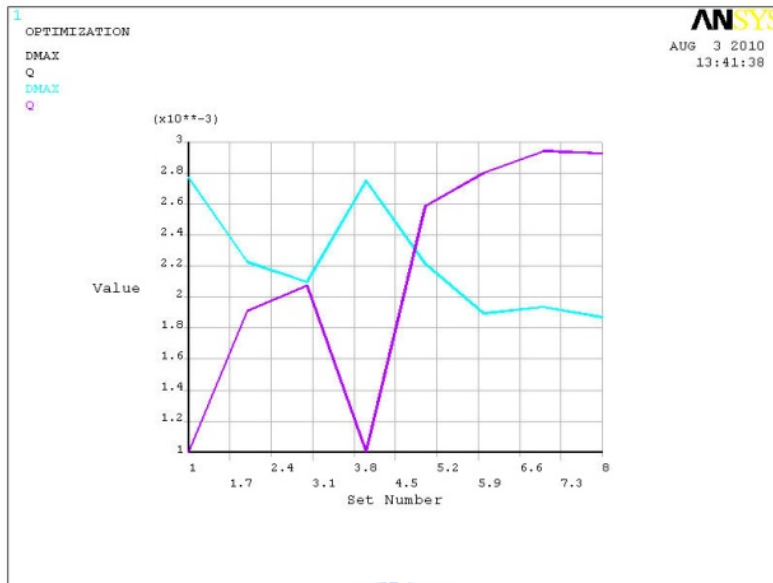


Fig. 29 Iteration process of Q and $DMAX$ (N=10)

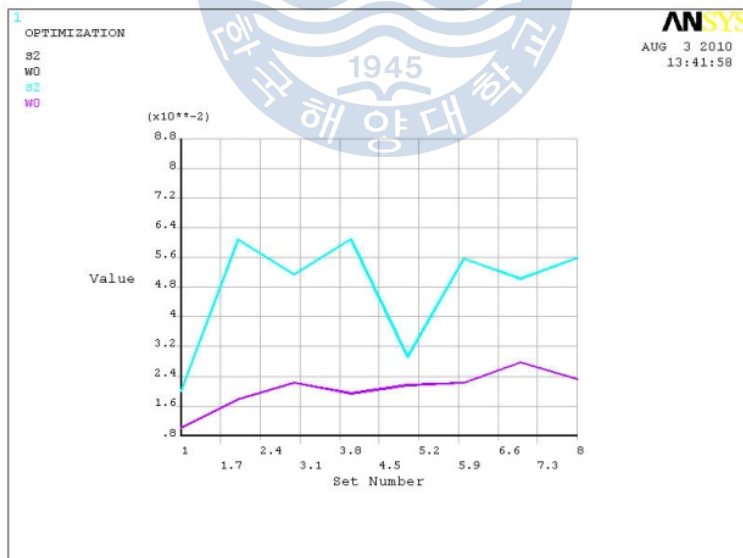


Fig. 30 Iteration process of W and S (N=10)

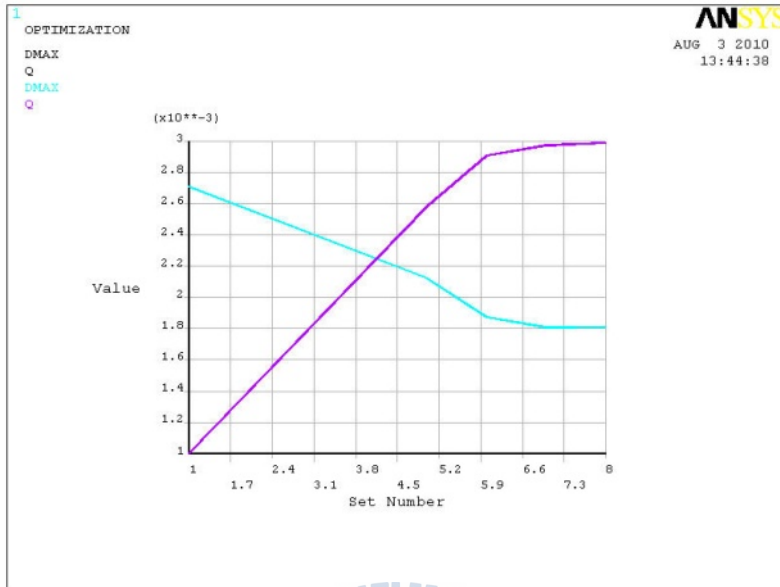


Fig. 31 Iteration process of Q and $DMAX$ (N=12)

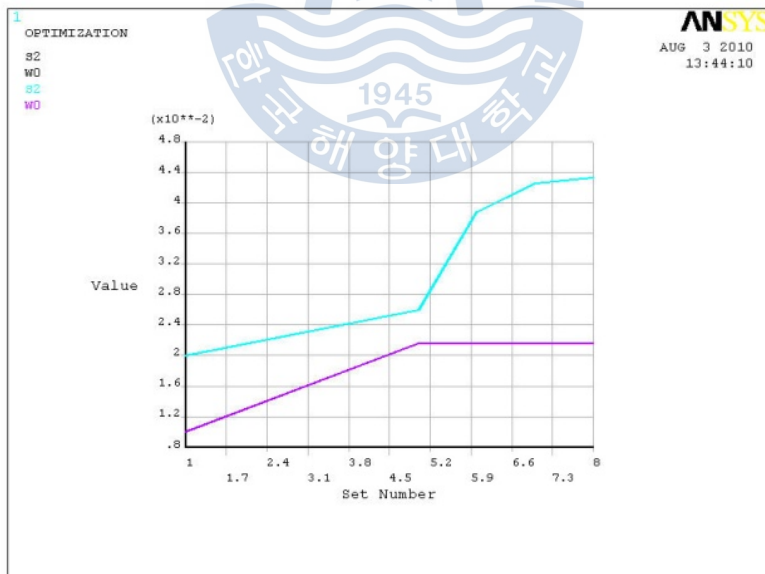


Fig. 32 Iteration process of W and S (N=12)

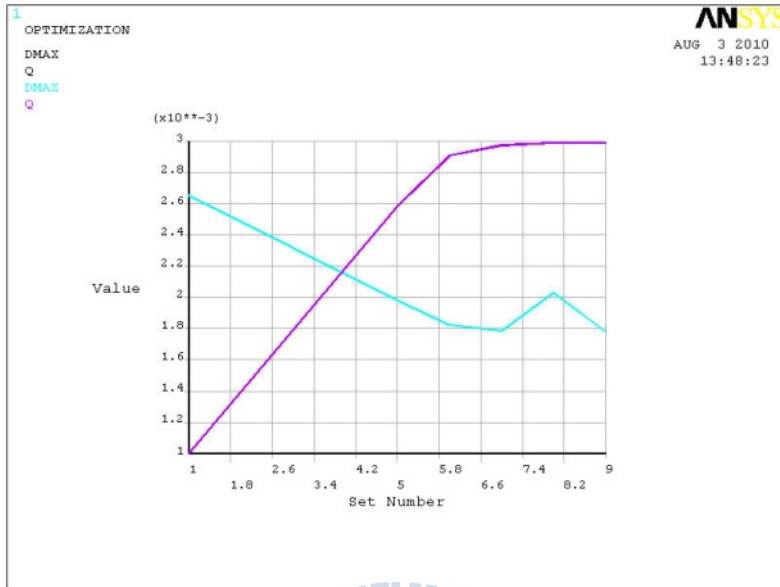


Fig. 33 Iteration process of Q and $DMAX$ (N=14)

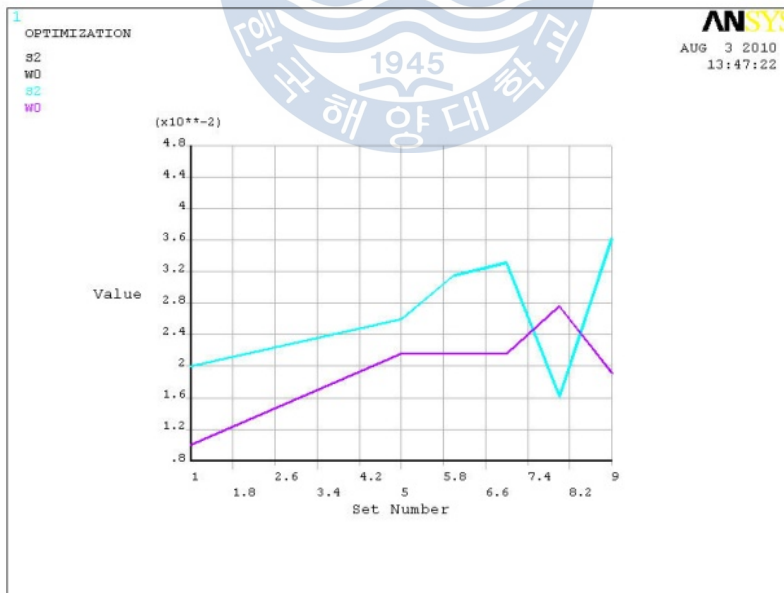


Fig. 34 Iteration process of W and S (N=14)

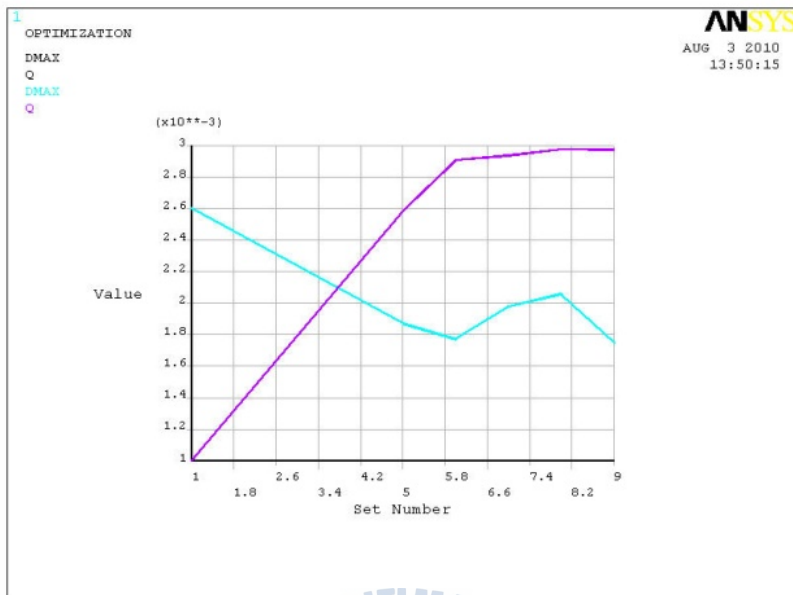


Fig. 35 Iteration process of Q and $DMAX$ (N=16)

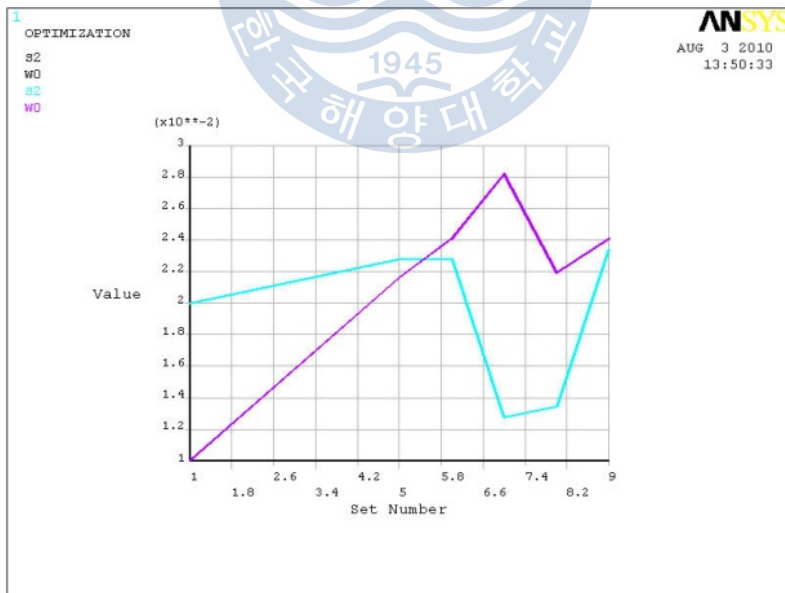


Fig. 36 Iteration process of W and S (N=16)

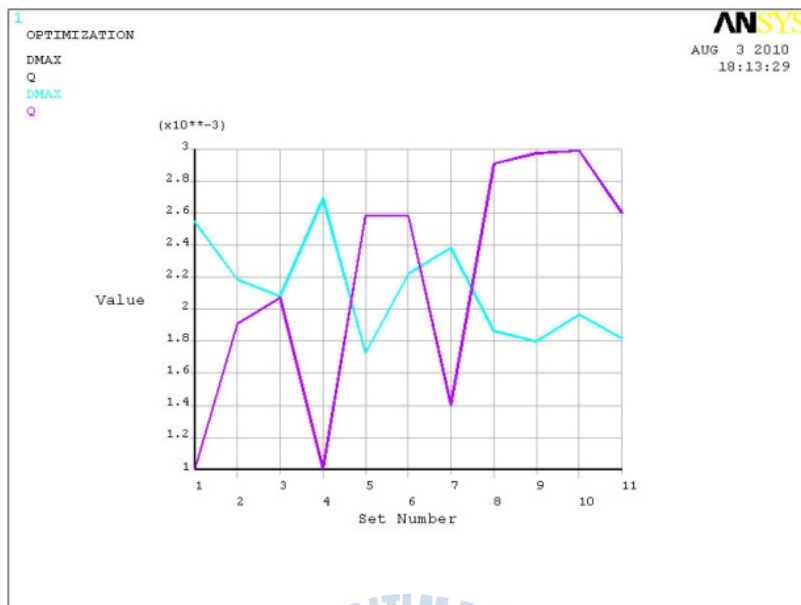


Fig. 37 Iteration process of Q and $DMAX$ (N=18)

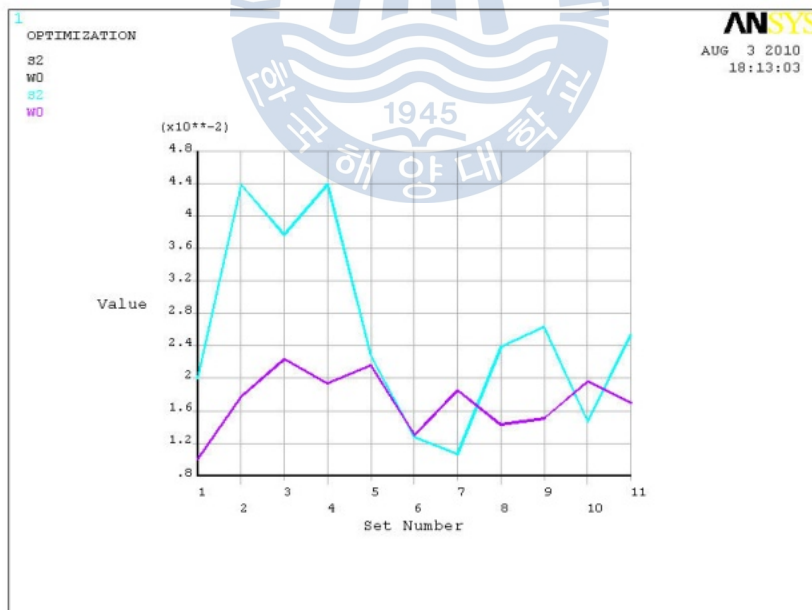


Fig. 38 Iteration process of W and S (N=18)

From the analysis results, we can see that, when plaque number was set to be constant, among the three design variables, plaque depth had the most obvious effect on refrigerator thermal deformation. Among the value rang of plaque depth, if plaque depth value approached upper limit of 3mm, refrigerator thermal deformation tended to decrease obviously. That was because plaques act as small hinges, permitting planar surface expansion without causing bowing of the cabinet. In addition, the plaques increased the structural rigidity of the liner and therefore resist thermal bowing. However, the plaque depth had better not exceed 3mm for the reason of design and aesthetics. The optimal plaque width and interval distance value were also different according to different plaque numbers in refrigerator inner case.

Comparing the analysis results with different plaque numbers, thermal deformation value approach the minimum when plaque number was sixteen, which was accordant with the result of the first optimization analysis process.

The optimization results showed that the optimal plaque parameters were when plaque number is sixteen, width was about 20~25mm, depth was about 3mm, and interval distance was about 22~28mm for the refrigerator model in this studying. The minimum thermal deformation was about 1.76mm. Engineers will be able to select optimal plaque parameters according to the previous analysis results for the design intensity and aesthetics.

3.4 Structural Optimization Using Artificial Neural Networks and Genetic Algorithm

The complexity of implementation of structural optimization numerical methods, the need for derivatives, and the deterministic and exhaustive nature, have made MP less attractive. Consequently research has been oriented in the direction of improving the above techniques and /or perhaps finding better approaches of dealing with the aforementioned problems in structural optimization. Soft computing techniques such as the GA were found to behave efficiently over a wide range of applications, even when employing numerous design variables and constraints.

GA was suggested by professor of Holland of Michigan University of Michigan in 20 century ^[31]. GA provides a method for solving complex optimizations of generic frameworks that do not rely on specific areas, GA is highly robust, so is widely used in the function of portfolio optimization, production scheduling, automatic control, image processing, machine learning, etc. Compared with traditional methods of optimization, GA with low requirements on the handling of various types of objective functions and constraints can be convenient and particularly has probabilistic sense of global search.

Goldberg is a pioneer in the work of GA and Samtani was the first to employ GA for structural optimization ^[32~33]. Most truss problems have and continue to be well studied using the GA method still now ^[34 ~ 39]. GA method is quite different compared to ANSYS optimal analysis. GA would start from many points by utilizing selection, crossover and mutation operators so that local convergence could be avoided. There is no special restriction for functions of the calculating model by GA because it does not need to obtain the derivative of the function, which would save a lot of computing time and improve the computing rate. GA is more suitable for complicated structure optimal projects than any

other traditional computing method in these days.

ANN is an empirical modeling tool analogous to the behavior of biological neural structures and can identify highly complex relationships by using input-output data ^[40]. Combined with the FEM technique, we set up the complex nonlinear relationships by utilizing a BP network, which would be the object function in a GA optimization.

In this study, we first obtained the refrigerator thermal deformation analysis data in ANSYS with different plaque parameters which are arranged in orthogonal test method, and then we trained the BP network in MATLAB by inputting the previous analysis data in order to find out the relationship between refrigerator thermal deformation and plaque parameters. Finally, the GA method was utilized to obtain the optimal plaque parameters for minimum refrigerator inner case deformation. The training data were obtained by the FEM model utilizing ANSYS because of the lack of experimental data. A total of forty-five FEM models were analyzed among which twenty-five models were arranged by the orthogonal test method according to plaque's depth (D), width (W) and interval distance (S). The FEM analysis results of thirty-eight models were input as training data and the other seven were taken as test data after a BP network training process in order to know how perfect the predicting model obtained by ANN training would match with the actual FEM analysis results.

BP-GA structural optimization analysis is to:

- 1) Set up relations between design variables, object function and constraints by using BP mapping method.
- 2) Implement optimal global searching using GA, and fitness of GA could be obtained by BP network.

The process of structural optimization is as following:

- 1) Define design variables, object function and constraints;
- 2) Make up a training sample set and test sample set by FEM analysis;

- 3) Train the BP network;
- 4) Implement optimal global searching for structural optimization;
- 5) Test the optimal results using test samples.
- 6) Optimization analysis using GA.

3.4.1 Parametric Analysis Interface based on Visual Basic

In the analysis of refrigerator deformation under thermal stress, usually we need to make a lot of models for different plaque parameters on the wall. Although ANSYS is a powerful universal software, which has powerful preprocess, solution and post process function, it takes us a lot of time and a lot of errors would inevitably be made as a result of human error in the modeling processes, APDL is easy for engineers to take parametric analysis and avoid repeating operations; however, APDL doesn't provide us with a graphical interface which would increase the difficulty in modeling and analysis process for the engineers.

VB is a very popular visual development tool/application program. More and more engineers are studying on the integrated development of VB and other software because of its powerful function and easily being learned and its ease of use^[41]. In order to make a series of analysis of refrigerator plaque modeling, we developed a method of parametric analysis based on VB, realized seamless integration of the two software application and increased analysis efficiency.

We make parametric modeling using APDL so that the parameters are easily modified including the material properties. VB provides the visual parameter input interface which would be delivered into ANSYS and text commands would be formed and executed by choosing different analysis functions as illustrated by the three buttons in the lower right corner of Fig. 39. We only need to input the parameters and press thermal or stress analysis function command buttons in an executable program which were created by VB, and then

return to the ANSYS interface to take thermal or stress analysis

VB software is a programming environment used to create graphical applications for the Microsoft Windows family of operating system. Unit exploitation of VB and ANSYS could effectively improve the parametric analysis efficiency and sufficiently embody specialization, customerization and facilitation. Usually there are two way to combine VB and ANSYS together. One is to call ANSYS by VB in the background, in which we should design a parametric modeling analysis text command file, then call the text command file using read and write functions with VB to finish analysis process ^[42]; The other way is to generate a parametric macro file in the ANSYS working directory by VB and run the macro file in ANSYS interface ^[43]. Although the preceding way could make full use of VB favorable advantages, we are not able to know what would happen in the background and would not be able to stop the analysis process until the end of run if there is something wrong, which would cost a lot of time. So we suggest using the second way to develop a very simple interface with VB and run the analysis process in ANSYS interface.

Macro files could be created and modified by any text editor. Usually we save it as *.mac file in ANSYS working directory. The working directory is usually at “C:\Program Files\Ansys Inc\v120\ANSYS\APDL”. We should also need to find this directory and open the “start120.ans” file to add a macro file name to the end of it. Close and save “start120.ans”; then the macro file operating button would be automatically created in ANSYS tool bar at every time we run ANSYS program.

In order to indicate the geometric parameters clearly for the users to input, we put an illustrative diagram in the interface as showing in Fig. 39. The source program for interface based on VB consists of two parts. One is developed for the thermal analysis process and the other for the structural analysis process. Both of which would generate corresponding macro file in ANSYS working directory after pressing running buttons.

The APDL file of parametric thermal analysis only defines the representative codes for

parameter; however we have to combine the data inputted in VB interface to such codes. So there are some commands that must be written in VB and we combined them with the APDL files of thermal analysis process. We have to note that the macro file has to be outputted into ANSYS working directory while using the APDL parametric file in VB working directory, otherwise the program would not run correctly.



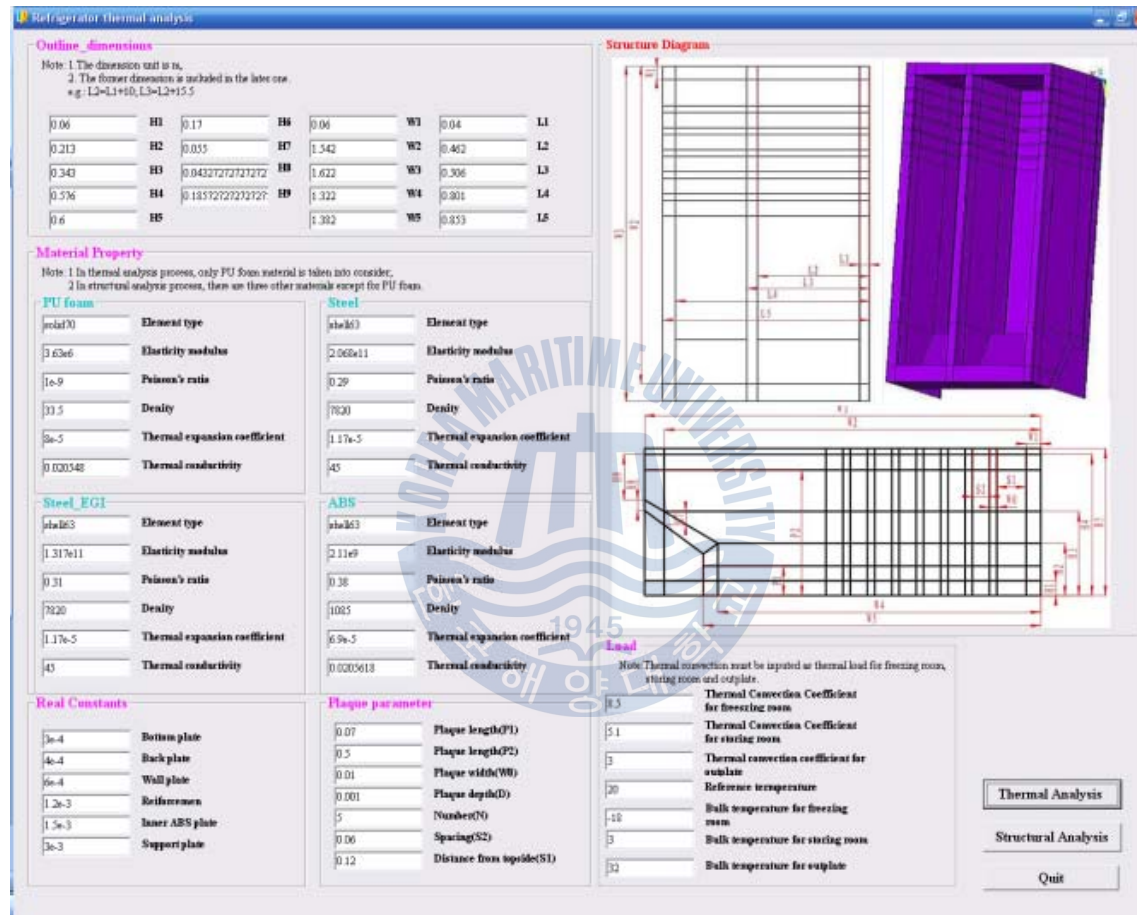


Fig. 39 Parametric analysis interface based on VB 6.0

3.4.2 Data preparation for training BP network

Orthogonal test is a design method for researching multi factors and levels. Since various parameters affect the analysis process, the orthogonal test table of $L_{25}(3)^5$ was designed to detect the most suitable extraction conditions of the three factors (plaque depth, plaque width and interval distance) for analysis data, as shown in Table 18.

Table 18 Factors and levels of orthogonal test

unit: mm

Variables	Level				
	1	2	3	4	5
D	1	1.5	2	2.5	3
W	10	12	15	18	20
S	20	30	40	50	60

Table 19 listed the data arranged by orthogonal test method. In order to add more analysis data so that the BP network would avoid local convergence, the additional thirteen of FEM analyses data were prepared as listed in Table 20. Table 21 listed the seven data for testing BP network.

Moreover, another seven sets of the additional FEM models have been prepared for testing of the ANN training model. Such test data would be compared with the predicting results by ANN model that we obtained in the training process.

Table 19 Orthogonal test data

(Unit:mm)	Depth	Width	Interval Distance	DMAX
Test-1	1	10	20	2.771
Test-2	1	12	30	2.745
Test-3	1	15	40	2.711
Test-4	1	18	50	2.755
Test-5	1	20	60	2.751
Test-6	1.5	10	30	2.572
Test-7	1.5	12	40	2.478
Test-8	1.5	15	50	2.411
Test-9	1.5	18	60	2.435
Test-10	1.5	20	20	2.496
Test-11	1.8	10	40	2.42
Test-12	1.8	12	50	2.32
Test-13	1.8	15	60	2.286
Test-14	1.8	18	20	2.45
Test-15	1.8	20	30	2.364
Test-16	2	10	50	2.286
Test-17	2	12	60	2.213
Test-18	2	15	20	2.448
Test-19	2	18	30	2.347
Test-20	2	20	40	2.22
Test-21	3	10	60	1.984
Test-22	3	12	20	2.371
Test-23	3	15	30	2.247
Test-24	3	18	40	2.09
Test-25	3	20	50	1.927

Table 20 Additional test data

(Unit:mm)	Depth	Width	Interval Distance	DMAX
Test-26	1	20	45	2.712
Test-27	1.5	15	35	2.464
Test-28	2	18	35	2.298
Test-29	2	15	45	2.242
Test-30	1.8	18	45	2.269
Test-31	1.5	12	50	2.446
Test-32	1.2	16	40	2.578
Test-33	1.5	17	42	2.409
Test-34	1.5	16	50	2.406
Test-35	2	18	55	2.152
Test-36	1.3	16	33	2.558
Test-37	1.7	20	41	2.32
Test-38	2.1	16	45	2.214

Table 21 Data for testing BP network

(Unit: mm)	Depth	Width	Interval Distance	DMAX
Test-39	1.2	15	32	2.62
Test-40	1.4	17	34	2.499
Test-41	1.5	18	38	2.432
Test-42	1.6	19	40	2.373
Test-43	1.8	19	42	2.287
Test-44	1.9	18	43	2.257
Test-45	2	17	44	2.232

3.4.3 Introduction of BP Network

The field of neural networks can be thought of as being related to artificial intelligence, machine learning, parallel processing, statistics, and other fields. The attraction of neural networks is that they are best suited to solving the problems that are the most difficult to solve by traditional computational methods.

Back Propagation (BP) is the generalization of the Widrow-Hoff learning rule to multiple-layer networks and nonlinear differentiable transfer functions. Input vectors and the corresponding target vectors are used to train a network until it can approximate a function, associate input vectors with specific output vectors, or classify input vectors in an appropriate way as defined by the user. Networks with biases, a sigmoid layer, and a linear output layer are capable of approximating any function with a finite number of discontinuities.

Standard BP is a gradient descent algorithm, as is the Widrow-Hoff learning rule, in which the network weights are moved along the negative gradient of the performance function. The term *back propagation* refers to the manner in which the gradient is computed for nonlinear multilayer networks. There are a number of variations on the basic algorithm that are based on other standard optimization techniques, such as conjugate gradient and Newton methods. The Neural Network Toolbox™ software implements a number of these variations.

Properly trained BP networks tend to give reasonable answers when presented with inputs that they have never seen. Typically, a new input leads to an output similar to the correct output for input vectors used in training that are similar to the new input being

presented. This generalization property makes it possible to train a network on a representative set of input/target pairs and get good results without training the network on all possible input/output pairs.

(a) Character of BP Network

Stimulation is applied to the inputs of the first layer, and signals propagate through the middle (hidden) layer(s) to the output layer. Each link between neurons has a unique weighting value. Each neuron receives a signal from the neurons in the previous layer, and each of those signals is multiplied by a separate weight value. The weighted inputs are summed, and passed through a limiting function which scales the output to a fixed range of values. The output of the limiter is then broadcast to all of the neurons in the next layer. So, to use the network to solve a problem, we apply the input values to the inputs of the first layer, allow the signals to propagate through the network, and read the output values.

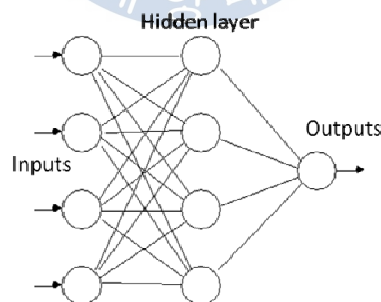


Fig. 40 BP network constitution

A BP network is highly nonlinear which does not need any mathematic expressions between inputs and outputs.

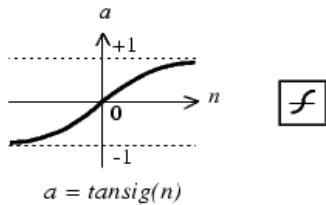
The BP learning process works in small iterative steps: one example case is applied to the network, and the network produces some output based on the current state of its synaptic weights (initially, the output will be random). This output is compared to the known-good output, and a mean-squared error signal is calculated. The error value is then propagated backwards through the network, and small changes are made to the weights in each layer. The weight changes are calculated to reduce the error signal for the case in question. The whole process is repeated for each of the example cases, then back to the first case again, and so on. The cycle is repeated until the overall error value drops below some pre-determined threshold. At this point we say that the network has learned the problem "well enough" - the network will never exactly learn the ideal function, but rather it will asymptotically approach the ideal function.

(b) Design of BP Network

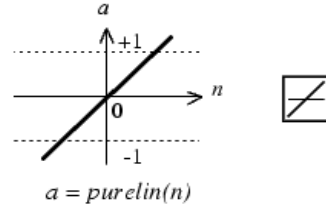
It's already proved that a network with bias comprised with at least one Sigmoid activation transfer function in a hidden layer and a linear output layer could be able to approximate any rational function. Usually the network precision could be improved by increasing hidden layers or neural units.

The activation function of a BP network should be differentiable anywhere. A tangent activation function '*tansig*' in a hidden layer and a linear activation function '*purelin*' in

the output layer are utilized in this study. The original weight value is usually selected as (-1, 1).



Tan-Sigmoid Transfer Function



Linear Transfer Function

Fig. 41 Function of tan-sigmoid activation

Fig. 42 Function of linear activation

Neural networks are suitable in many areas which contain a lot of complicated relations among variables, such as structural optimization analysis.

3.4.4 BP Application on Optimization

In structural optimization analysis, plenty of calculations for detailed structural analysis would greatly decrease efficiency of optimization design, especially in the complicated optimization analysis. Usually, the expression for relationship between design variables and state variables, or object functions is so complicated that it is impossible for engineers to give out the explicit equations. Back-propagations neural network is suitable to set up such complicated non-linear relationship by using neural network mapping method.

This paper applied BP Neural Networks ^[44] in MATLAB V7.0. A common ANN model was established in a training process by using BP with the Gradient Descent (GD) algorithm. The structure of the BP network includes three layers: an input layer, a hidden

layer and an output layer,. The input layer receives three input parameters (D, W, and S) of the refrigerator plaque and the output layer provides the output of the deformation, which is shown as the following Fig. 43:

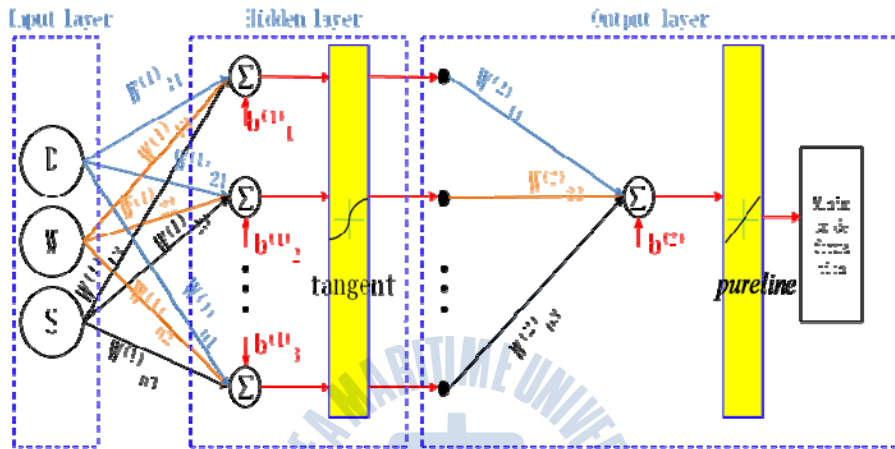


Fig. 43 The ANN structure

The input D, W and S have boundary as the following:

$$1 \text{ mm} \leq D \leq 3 \text{ mm};$$

$$10 \text{ mm} \leq W \leq 20 \text{ mm};$$

$$20 \text{ mm} \leq S \leq 60 \text{ mm}$$

However, during the FEM analysis process, our purpose was to find out the maximum inner case deformation, which would be collected as the input data for training the BP network. For the BP network, we wanted to know under what condition of the D, W and S parameters that the minimum inner case deformation would emerge. The minimum inner case deformation is the final goal of our optimal structure design, and the regular pattern between the three design variables and the minimum inner case deformation is what we

wanted to find out by training the BP network to obtain a reliable ANN model.

With the specified transfer functions ‘tangent sigmoid’ and ‘pureline’, the unknown function relationship between input of ‘D’, ‘W’, ‘S’ and outputs of ‘minimum deformation’ could be determined iteratively along with the iterations of the weights $W^{(1)}$ and $W^{(2)}$, and biases $b^{(1)}$ and $b^{(2)}$. By learning the patterns of these inputs and outputs, the weights and biases were adjusted iteratively during the training procedures.

3.4.5 BP Network Training Results

After about 2000 steps calculations, the ANN mathematical predicting model that describes the mapping relation between three refrigerator structure parameters and refrigerator deformation was given by the following matrix.

$$a^{(2)} = \sum \log \operatorname{sig} \sum \begin{bmatrix} 1.238792 & 1.165185 & 1.219723 \\ 1.041236 & 2.627182 & 2.245848 \\ 2.256535 & 1.556408 & 1.284563 \\ 2.807582 & 1.921486 & 1.000731 \\ 2.069445 & 2.799104 & 1.156337 \\ 1.680374 & 2.589023 & 2.799691 \\ 2.347242 & 1.668423 & 1.263368 \\ 1.905393 & 2.658961 & 2.588985 \\ 2.319821 & 1.92195 & 2.23715 \\ 1.876695 & 2.815351 & 2.95049 \\ 1.837282 & 2.319985 & 1.730943 \\ 2.889831 & 2.542241 & 2.849636 \\ 1.572581 & 1.514649 & 1.418931 \\ 2.691162 & 1.879647 & 1.221641 \\ 1.646999 & 1.423261 & 1.615893 \\ 2.64171 & 1.678898 & 2.658364 \\ 1.303184 & 2.28118 & 2.036388 \\ 2.583637 & 2.787595 & 2.680989 \\ 2.7268 & 2.469997 & 1.33453 \\ 1.789515 & 2.51745 & 1.423039 \end{bmatrix} \times [D \ W \ S] + \begin{bmatrix} 2.971556 \\ 1.006559 \\ 2.32273 \\ 2.213407 \\ 1.605572 \\ 1.334885 \\ 1.975103 \\ 2.371402 \\ 1.397904 \\ 2.011912 \\ 2.079205 \\ 1.276939 \\ 2.548614 \\ 2.822303 \\ 2.18899 \\ 2.41698 \\ 2.260864 \\ 2.187141 \\ 2.480579 \\ 1.539709 \end{bmatrix} \times \begin{bmatrix} 1.658191 \\ 1.414538 \\ 1.006845 \\ 1.618149 \\ 1.640824 \\ 1.419829 \\ 1.07136 \\ 1.573235 \\ 1.064027 \\ 1.27787 \\ 1.01407 \\ 1.163589 \\ 1.1405 \\ 1.093756 \\ 1.116828 \\ 1.704792 \\ 1.843791 \\ 1.652464 \\ 1.593323 \\ 1.025109 \end{bmatrix}^{-1} + [1.0032]$$

After the training process, the general ability of the ANN model must be tested by using seven sets of random combinations of testing data shown in Table 22, showing the comparison between predicting data predicting data computed from the FEM computed results for the test data. In addition, the maximum error of the ANN model is -0.49%. Such an ANN model was thought to be a reliable mathematical model in predicting the effect of plaque parameters on refrigerator inner case deformation.

Table 22 Test result

Unit: mm Number	Depth	Width	Interval distance	Test result	FEM result	Error (%)
Test-39	1.2	15	32	2.6084	2.62	0.44
Test-40	1.4	17	34	2.5002	2.499	-0.05
Test-41	1.5	18	38	2.4439	2.432	-0.49
Test-42	1.6	19	40	2.3809	2.373	-0.33
Test-43	1.8	19	42	2.2893	2.287	-0.11
Test-44	1.9	18	43	2.2584	2.257	-0.06
Test-45	2.0	17	44	2.2242	2.232	0.35

3.4.5 Structural Optimization Analysis of Refrigerator Using Genetic Algorithm

After the nonlinear mapping between plaque parameters and refrigerator inner case deformation has been established using the BP neural network training algorithm, the desired target function approximation value for plaque parameter optimization could be obtained by genetic algorithm.

GA has been widely applied in many areas, such as control, prediction, forecasting,

optimization, differentiation, vision, etc. The use of GA has become popular in recent years to optimize the structure parameters and obtain optimal structure design parameters in the engineering, including applications of the BP artificial neural network and GA to the parameters optimization of profile extrusion die^[45], optimal laser-cutting parameters for QFN packages by utilizing artificial neural and genetic algorithms^[46]. And the die shape in extrusion^[47], and the optimal output feedback controller^[48] and controller parameters of heating ventilating and air conditioning^[49].

The steps for genetic algorithm learning are as follows:

- (1) Initialize population-P, including crossover scale、crossover probability-Pc、mutation probability-Pm as well as any WIH_{ij} and WHO_{ji} ; In coding, using real-coded style, initial population from 50;
- (2) Compute every individual assessment function, and sort them ; select the network individuals according to the following equation:

$$p_s = f_i / \sum_{i=1}^N f_i$$

In which, f_i is individual adaptation value, to judge by the error quadratic sum-E as following:

$$f(i) = 1/E(i) \quad E(i) = \sum_p \sum_k (V_k - T_k)^2$$

In which, $i=1, \dots, N$ is the chromosome number; $k=1, \dots, 4$ is the node number of output layer; $p=1, \dots, 5$ is sample number for learning; T_k is teacher signal.

- (3) Generate new individuals G'_i and G'_{i+1} by crossover operation on individuals of G_i and G_{i+1} with probability of Pc, copy directly the individuals which didn't take

crossover operation;

- (4) Generate new individual G_j' from old individual of G_i by mutation with probability P_m ;
- (5) Insert all the new individuals into population P and calculate the evaluation function for new individuals;
- (6) If the satisfied individual, then end, otherwise, turn to step (3).

Obtain the optimal network connection weights by decoding the optimal individual in the final population after results reach the performance indicators.

In this study, we used the GAOT toolbox by Christopher R. Houck of MATLAB in 1996. Using GAOT, designers do not have to consider of genetic algorithm internal structure, only work on the fitness function program according to the design requirements. So GAOT toolbox simplified the originally complex genetic algorithm design process, which has been proved very helpful for numerical optimization.

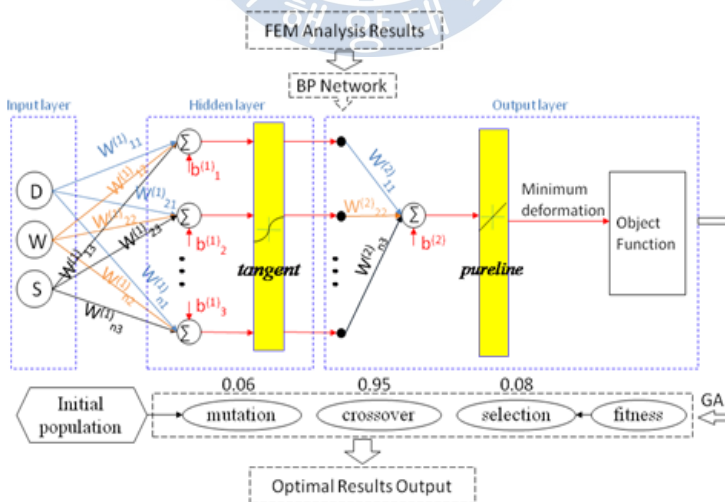


Fig. 44 GA process

3.4.6 GA Optimization Results

The error between the two results is very small, and the optimization result by the GA method is thought to be reliable. Fig. 45 shows the regular pattern between plaque parameters and refrigerator minimum deformation. Fig. 46 shows the FEM analysis result by GA optimal data. Fig. 47 shows the max deformation on the wall between freezing inner case and outside. Fig. 48 shows the max deformation of model without plaques.

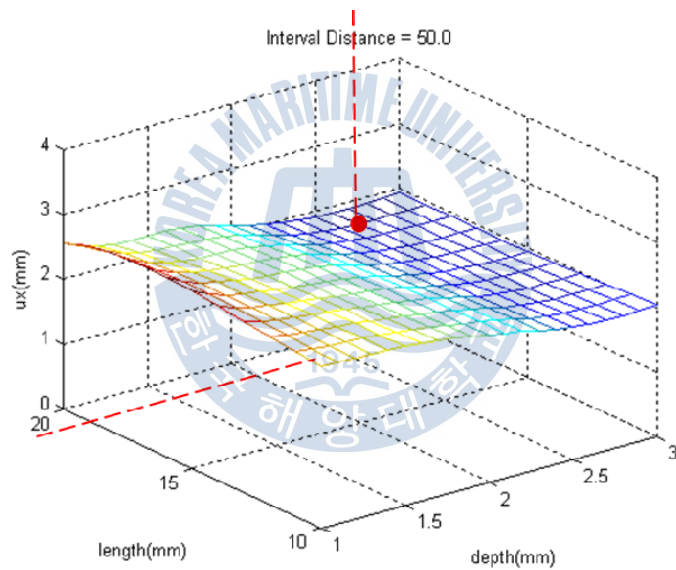


Fig. 45 Result of GA optimization analysis

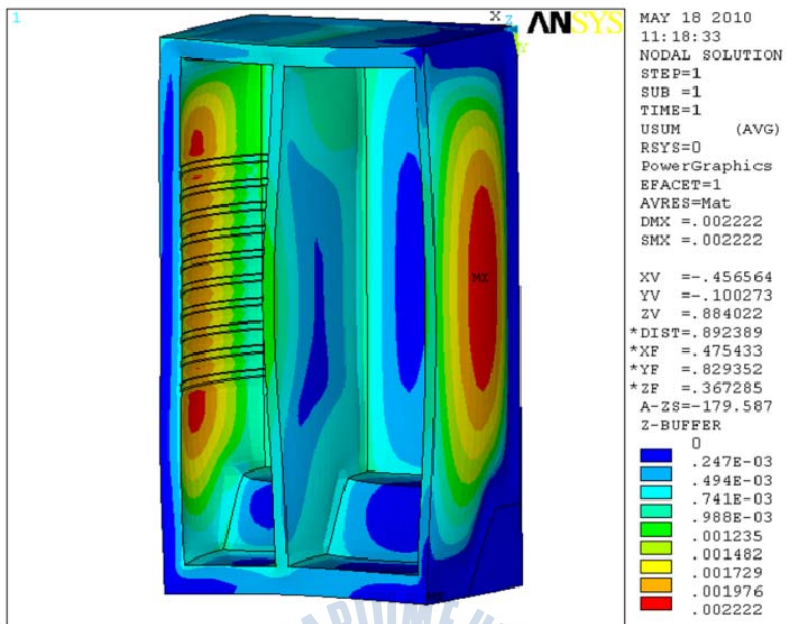


Fig. 46 FEM analysis result with GA optimization parameters

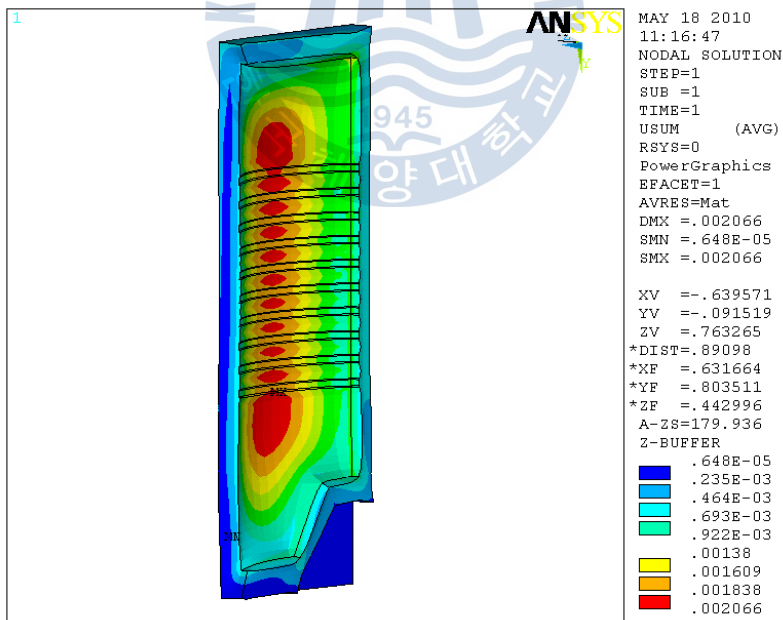


Fig. 47 MAX deformation of model with plaques

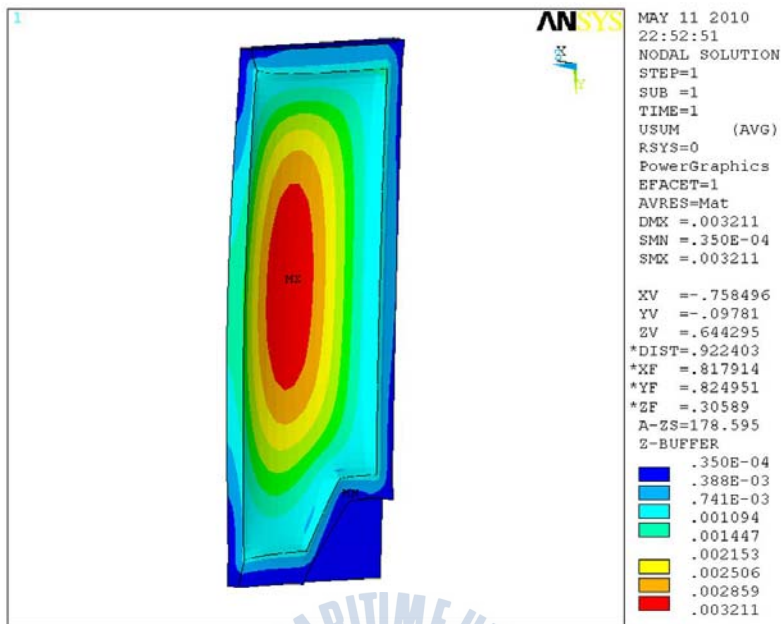


Fig. 48 MAX deformation of model without plaques

We made an FEM model with the GA optimization result of D, W and S, and obtained the FEM result of maximum inner case deformation, which is 2.066mm. The comparison of the FEM result and the GA optimization result is shown in Table 23:

Table 23 FEM and GA optimization result

GA optimization parameter for FEM model	FEM result in ANSYS	GA optimization result in MATLAB
D=2.627mm	2.066mm	1.9096mm
W=19.2396mm	Error	
S=49.3762mm		
	$(2.066-1.9096)/2.066 \times 100\% = 7.57\%$	

Compared to the unplaqued refrigerator model as shown in Fig. 48, the plaques distributed evenly along the inner case wall according to the optimization result, so that the

plaques separated the maximum deformation area to small areas with $S=49.38\text{mm}$ as shown in Fig. 46~47. As a result, the inner case deformation could also be effectively reduced. The inner case deformation of FEM plaque model could be reduced from 3.21mm of the unplaqued model to 2.07mm according to the optimization result.

The BP neural network has been applied to construct a mathematical model wherein the refrigerator inner case deformation function expressed as explicit nonlinear functions of the three structure parameters D , W and S . The established ANN model was trained from thirty-eight sets of the FEM analysis data and tested by the extra seven sets of the FEM analysis data. The maximum test error is 7.57% .

Finally, the GA was utilized to obtain the optimal structure parameters that provide the best refrigerator deformation quality. The best structure parameter was $D=2.63\text{mm}$, $W=19.24\text{mm}$, $S=49.38\text{mm}$, and minimum deformation was 1.91mm . The result of GA optimization was considered reliable, and the method for refrigerator structural optimization was practicable.

Chapter 4 New Design Concept of Refrigerator to Decrease Thermal Deformation

4.1 Introduction

Many deformations with refrigerators have inevitably arisen after foaming as a result of the flat area of inner case wall being too large or the foaming technological parameters not designed suitably. If the inner case is designed into a diamond shape, the deformations are anticipated to be avoided. However, in this study, we brought forth a new idea of pre-forming in order to decrease refrigerator cabinet thermal deformation. The pre-forming design can effectively reduce thermal deformation if the parameters are arranged suitably for various refrigerators.

4.2 Diamond Pattern Design

The diamond pattern was put into use recently in order to improve the exterior appearance which depends on the inner case after the foam is formed. The diamond shape will contribute to cold air distributing throughout the inner case space. The diamond shape increases cooling area and surface turbulence effect, and the diamond shape also increases the radiation heat transfer coefficient, which lead to lower temperature than models with bald wall ^[50]. Aesthetically, the diamond patterns will also beautify the inner case by diffusing scattered light.

In consideration of the above reasons, we designed several models with the diamond shape on the inner case wall in order to analyze the cooling effect and structure deformation.

4.2.1 Diamond Pattern Geometry

The diamond geometry is designed in hexagonal pyramid style shown in the following figures, which is shown as in Fig. 49.

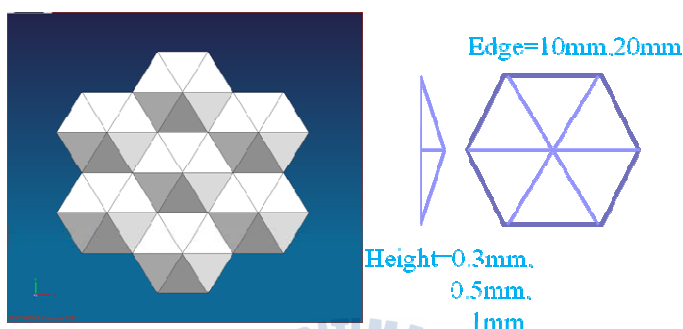


Fig. 49 Diamond geometry

The diamond pattern was designed separately in convex style and concave style, as shown in the Fig.50~51.

The diamond area is designed in part of the inner case wall except for pattern_5, shown in the following Fig. 52~53. We also designed a new plaque model in order to keep consistent with the refrigerator parameter of diamond patterns, as shown in Fig. 54. Parameters of the five models are listed in Table 24.

Table 24 Parameters of diamond models

	Edge(mm)	Height(mm)	Type
Pattern_1	10	0.3	convex
Pattern_2			concave
Pattern_3		0.5	
Pattern_4		1	
Pattern_5	20		

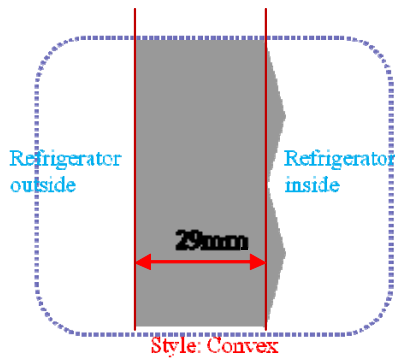


Fig. 50 Convex diamond

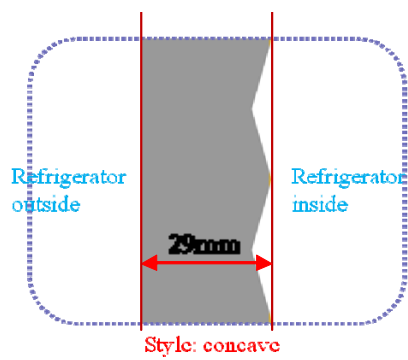


Fig. 51 Concave diamond

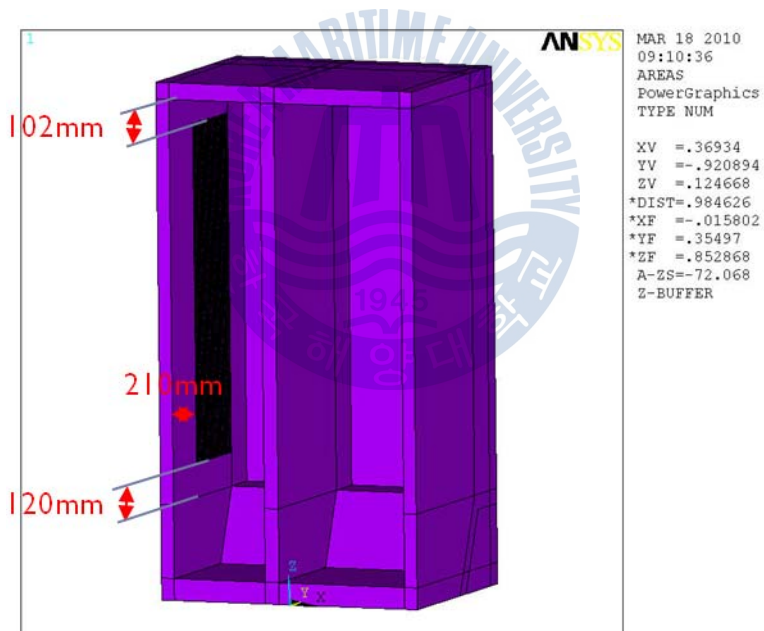


Fig. 52 Diamond area

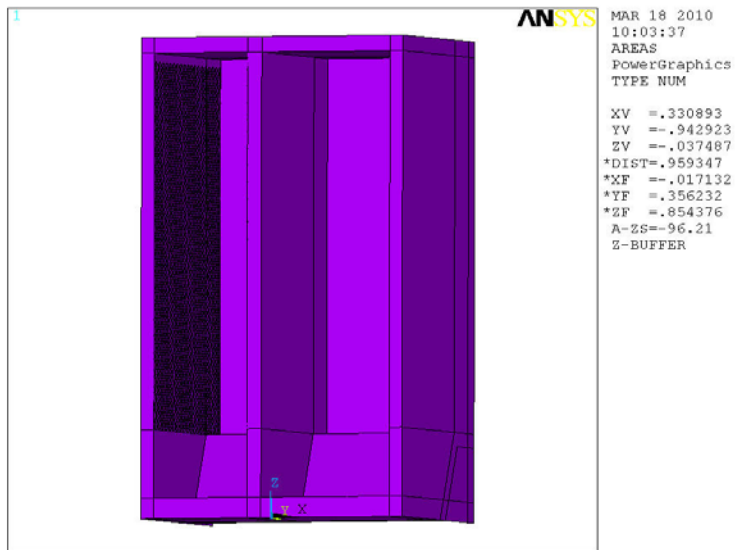


Fig. 53 Pattern_5

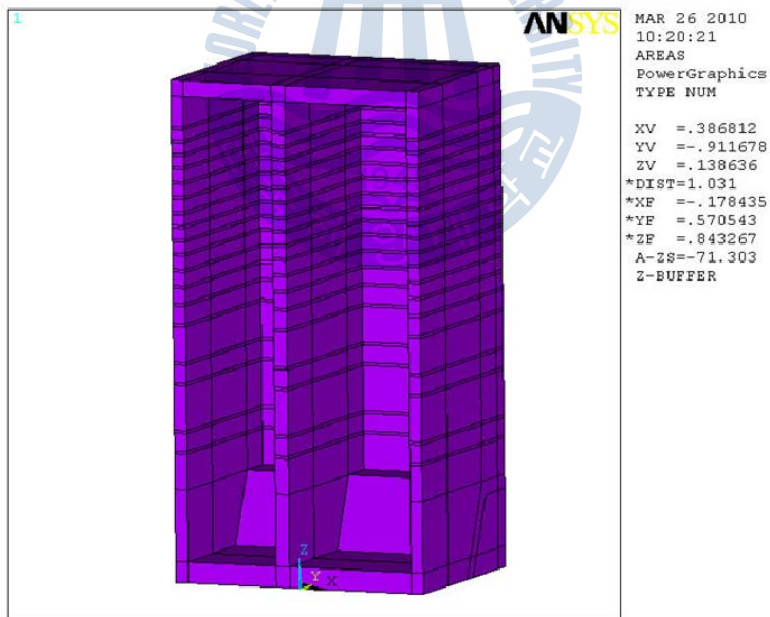


Fig. 54 Plaque model (Depth: 1mm)

4.2.2 Diamond Pattern Thermal Analysis Result

The analysis of the loading condition is as the same as that in previous chapters. After calculating, temperature distribution analysis results are shown in the Fig. 55~61.

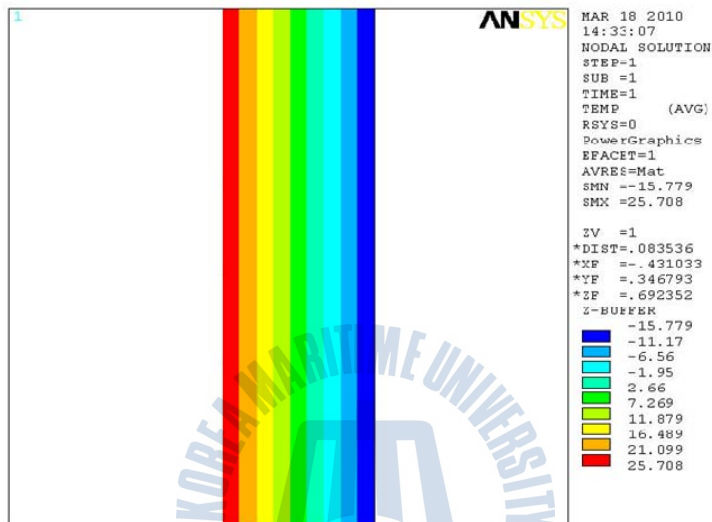


Fig. 55 Temperature condition of smooth model

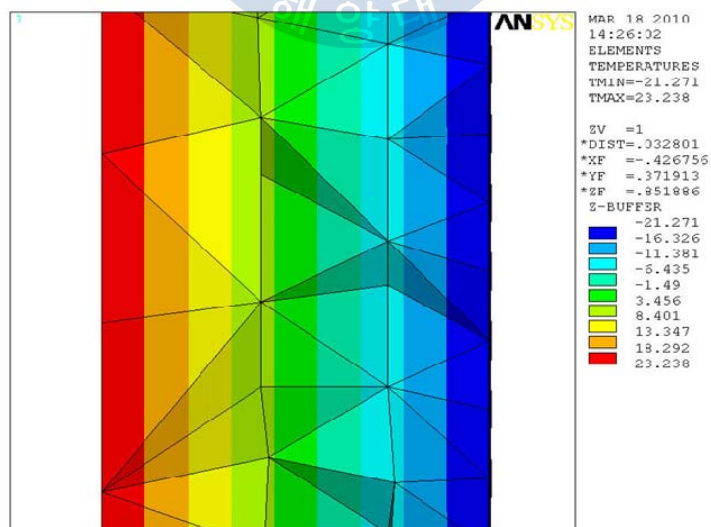


Fig. 56 Temperature condition of pattern_1

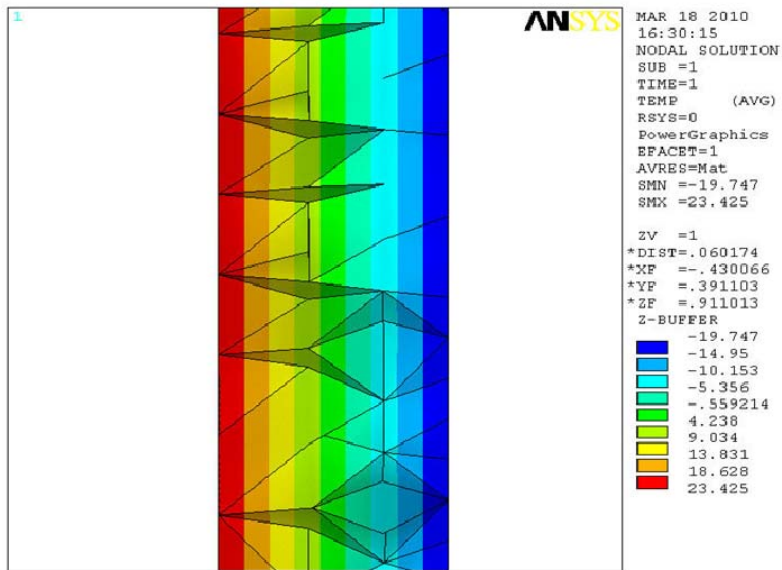


Fig. 57 Temperature condition of pattern_2

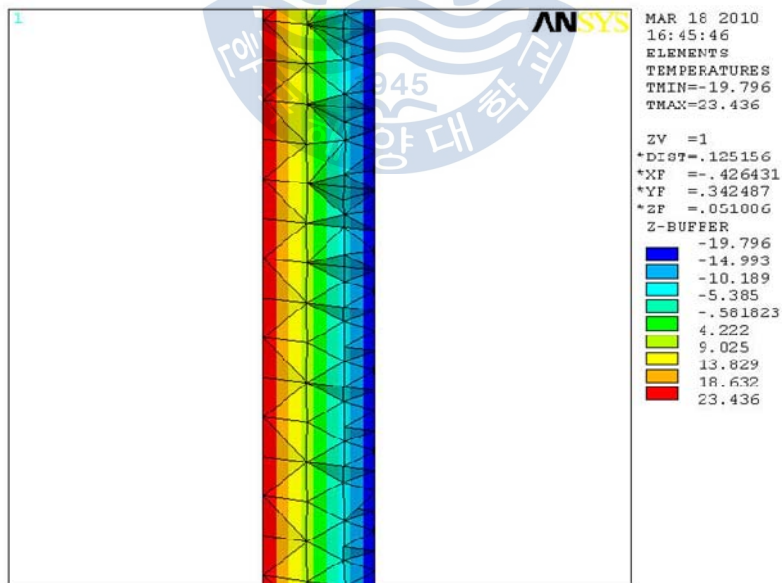


Fig. 58 Temperature condition of pattern_3

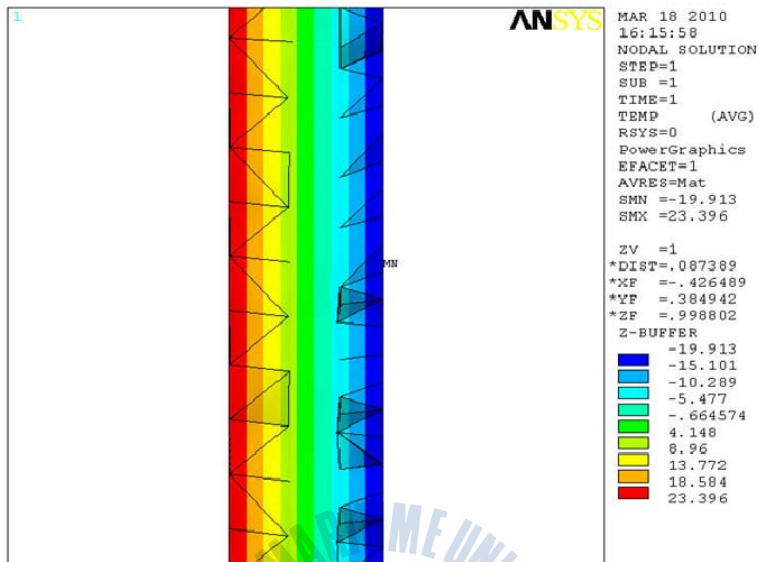


Fig. 59 Temperature condition of pattern_4

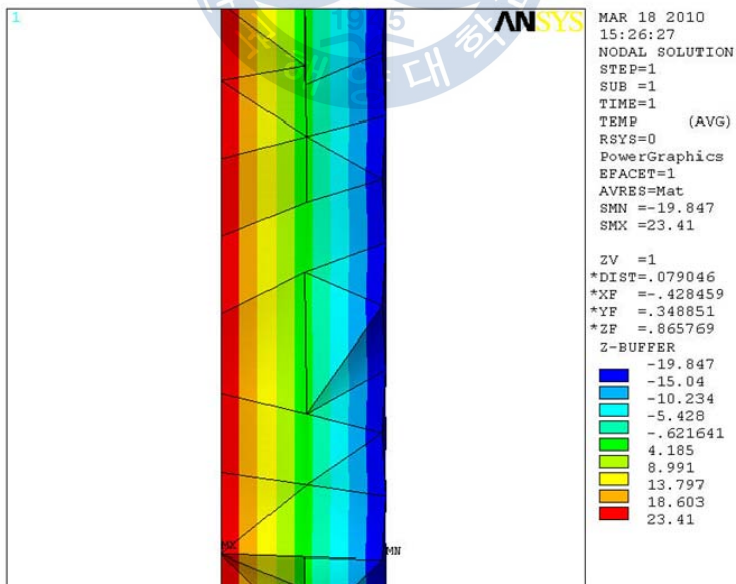


Fig. 60 Temperature condition of pattern_5

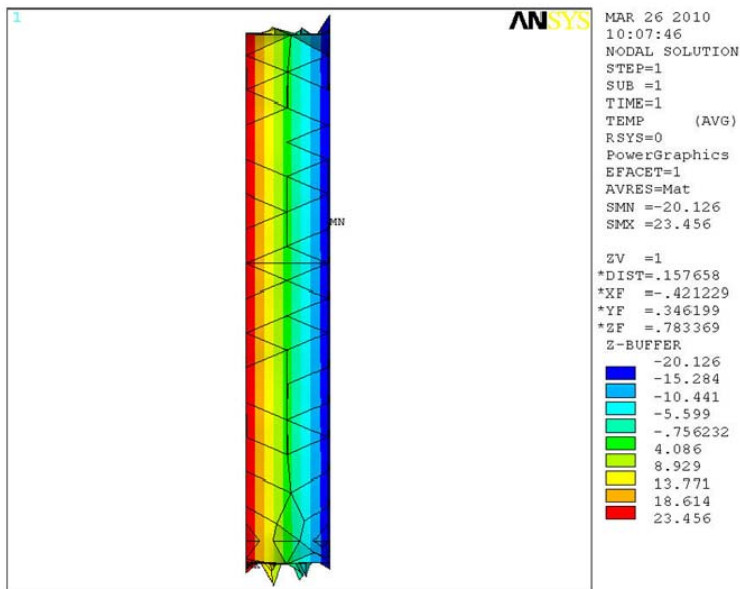


Fig. 61 Temperature condition of plaque model

The thermal analysis results are shown in Table 25. Thermal analysis results show that models with diamond or plaque would keep lower temperature in the freezing room than models with smooth inner case wall.

Table 25 The lowest temperature of models

	Inside(°C)	Outside(°C)
Smooth model	-15.78	25.71
Pattern_1	-21.27	23.24
Pattern_2	-19.75	23.43
Pattern_3	-19.80	23.44
Pattern_4	-19.91	23.40
Pattern_5	-19.85	23.43
Plaque model	-20.13	23.46

For uniform wall temperature, profiles of similar shape recur periodically. On the other

hand, for prescribed wall heat flux which is the same for all modules, the temperature field itself is periodic provided that a linear term related to the bulk temperature change is subtracted. Fluid flow direction change has played the role of heat transfer enhancement. Vortex fluid will occur after the fluid movement of inertia separates from the convex side ^[51]. Fluid impact on the concave side of the wall enables intensification of quality and momentum transfer and substitution between boundary layer fluid and mainstream fluid; as a result, heat transfer will be intensified both in convex side and in concave side.

In this study, we didn't take any fluent analysis, the reason for diamond and plaque models with lower temperature distribution is mainly because the change of the thickness of the wall.

4.2.3 Diamond Pattern Structural Analysis Result

After loading temperature condition, we took structural analysis process; the results are shown as in Fig. 62~68. Table 26 lists the deformations of the five models.

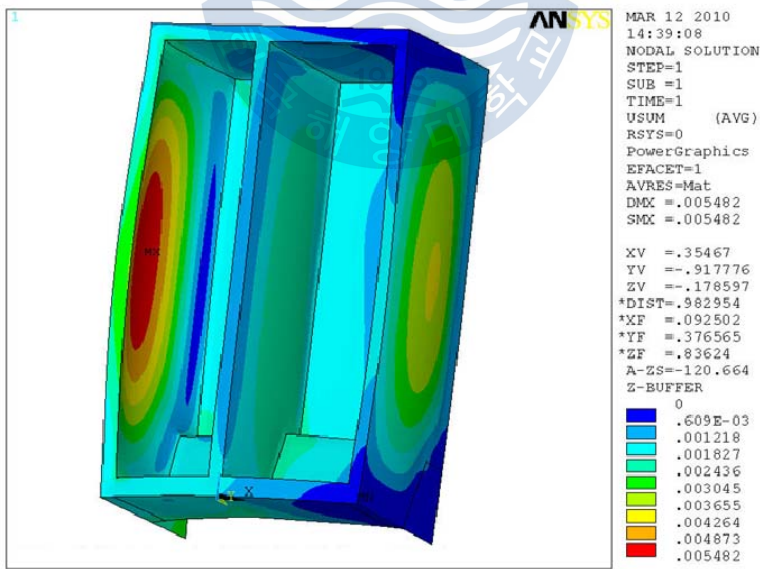


Fig. 62 Structural analysis result smooth model

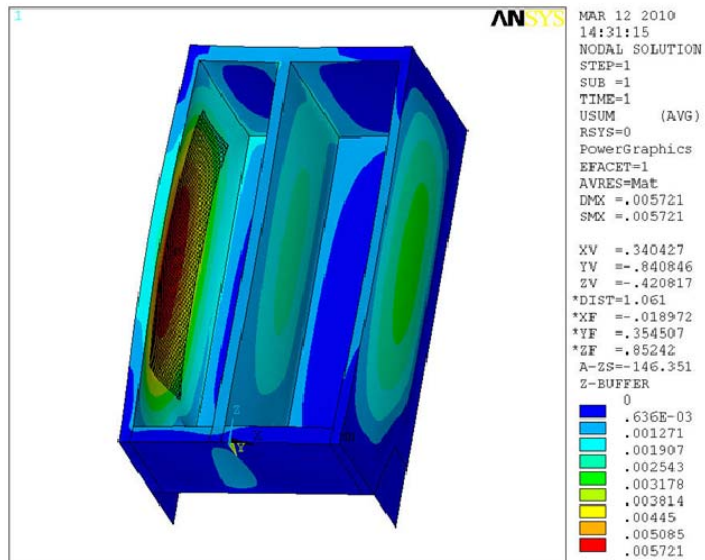


Fig. 63 Structural analysis result of pattern_1

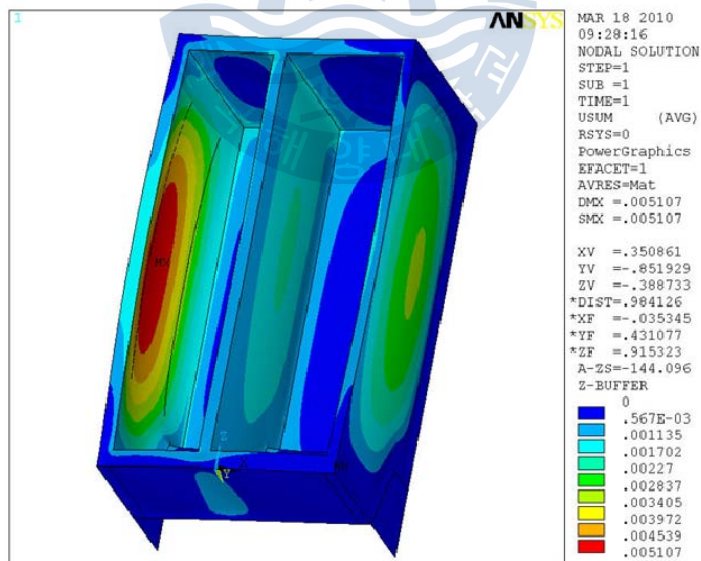


Fig. 64 Structural analysis result of pattern_2

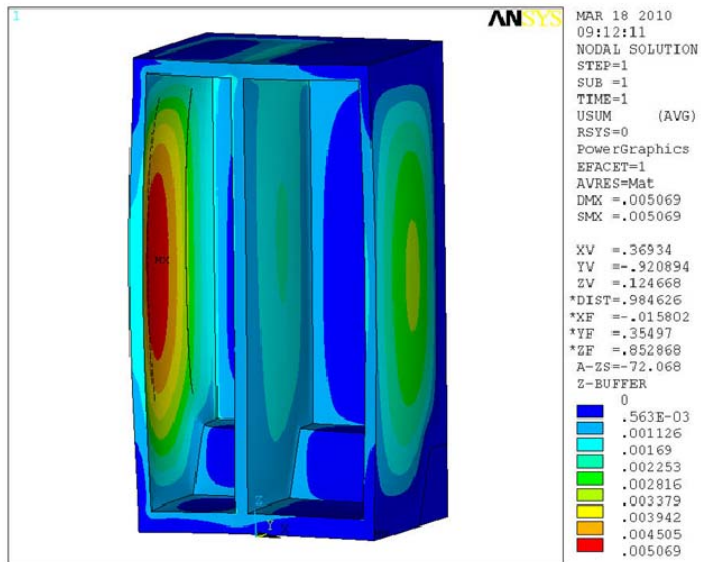


Fig. 65 Structural analysis result of pattern_3

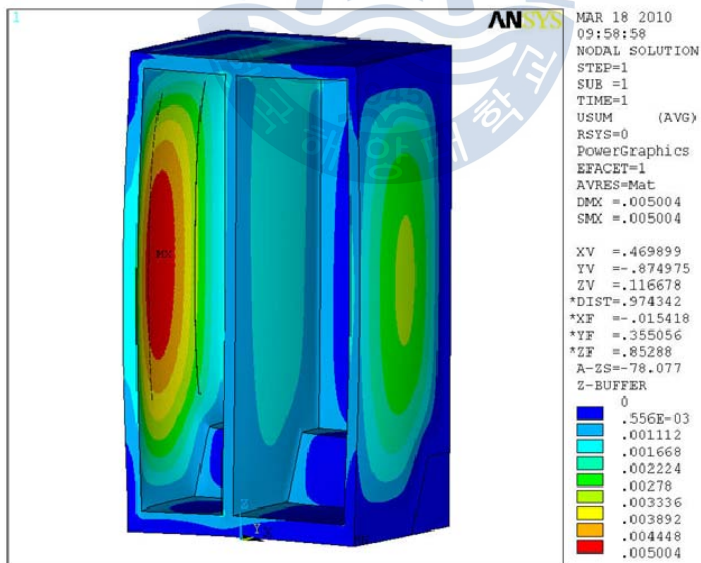


Fig. 66 Structural analysis result of pattern_4

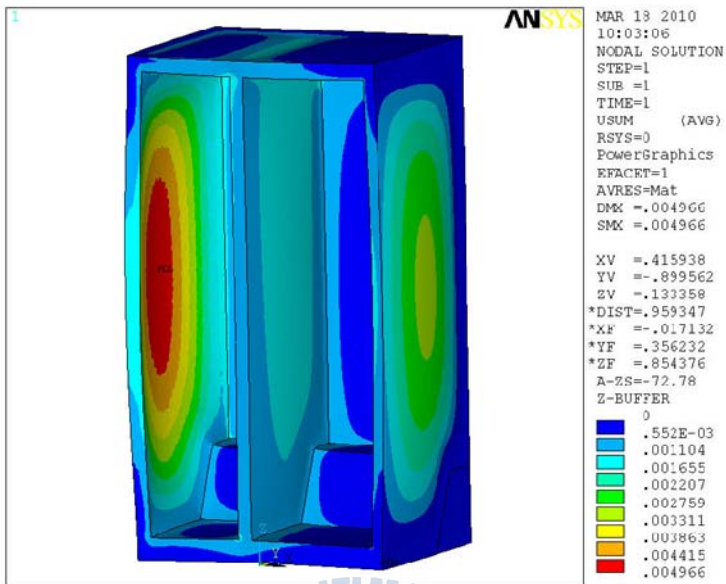


Fig. 67 Structural analysis result of pattern_5

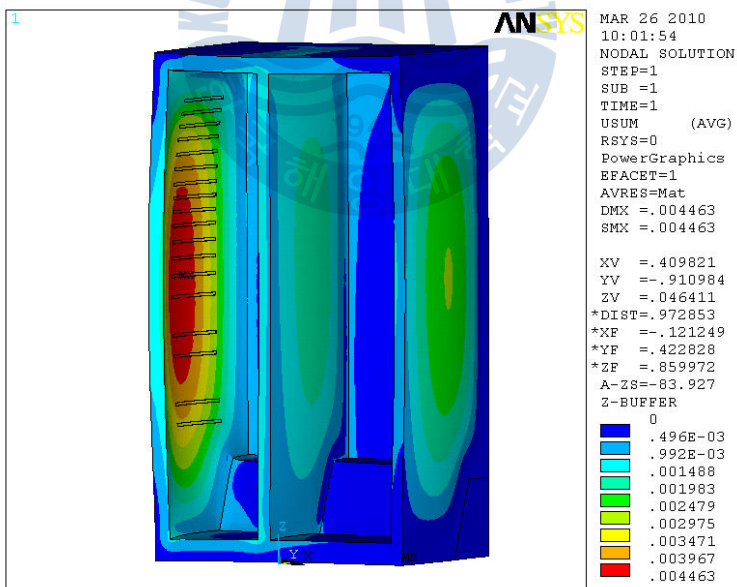


Fig. 68 Structural analysis result of plaque pattern

Table 26 Structural analysis result comparison of diamond models

	Horizontal Deformation (mm)
Without bead	5.48
Pattern_1	5.72
Pattern_2	5.11
Pattern_3	5.07
Pattern_4	5.00
Pattern_5	4.97
Plaque Model	4.46

From the analysis results, we can see that the plaque model could decrease refrigerator thermal deformation more than diamond patterns. Structural analyses results show that diamond pattern almost doesn't have any obvious effect on decreasing thermal deformation. So the diamond design is not suitable to decrease thermal deformation. However, the diamond pattern design would increase the cost of manufacture; we don't suggest the diamond pattern design from a mechanical design aspect.

4.3 Pre-Forming Design

As the previous analysis results, the temperature gradient which exists across the cabinet wall produces a bi-material effect, where the various materials in the cabinet wall expand or contract by a different amount in response to the temperature gradient. The interior plastic liner is exposed to the cooled interior of the refrigerator compartments, and the liner surface therefore tends to contract slightly. The exterior shell is exposed to a warm ambient temperature, and therefore tends to expand. Although the liner and shell surfaces respond differently to the thermal effects, they are locked together by the foam layer and may not move freely with respect to one another. As a result, the cabinet sidewalls tend to bow outward to compensate for the expansion and contraction of the different layers of the walls. The bowing is generally more severe in cabinet walls adjacent to the frozen food compartment than in those adjacent to the fresh food compartment due to the greater temperature gradient across the freezer compartment walls. Side-by-side refrigerators are more susceptible to cabinet bowing than top mount or bottom-mount cabinets because the side-by-side cabinet is divided vertically by a compartment separator wall, and lacks the horizontal divider of the top-mount or bottom-mount which to some extent ties the cabinet sidewalls together. Bowing of the cabinet sidewalls is of particular concern because the compartment shelves are sometimes mounted between the opposed sidewalls of the compartment, and when the cabinet bow is excessive the shelves are unable to span the increased distance and may collapse. Or in some cases thermal bowing will lead to dropping of the transverse shelves for goods. Other detrimental effects of cabinets bowing include misalignment of the cabinet doors and door seals, inactivation of door-actuated switches, and increased energy consumption due to air leakage around the doors.

4.3.1 Geometry of Pre-Forming Design

Based on the previous analysis results, we come up with the concept of pre-forming. According to the inward bowing characteristic of thermal deformation, we previously form the sidewall by a reverse deformation shape in some suitable extent. For the refrigerator model in this studying, the normal thermal deformation is about five mm; therefore, we designed the pre-forming pattern as shown in Fig. 69~72.

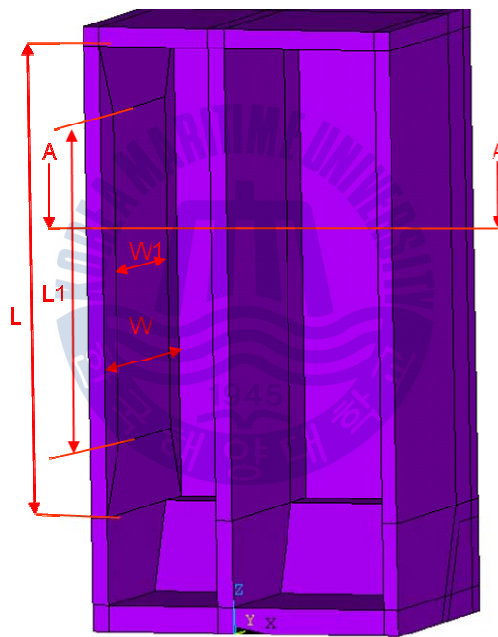


Fig. 69 Pre-forming area

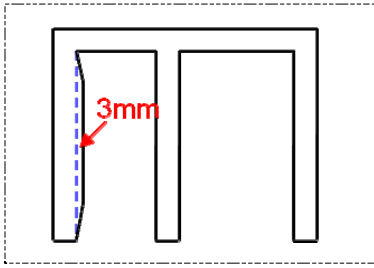


Fig. 70 Pre-forming of convex pattern

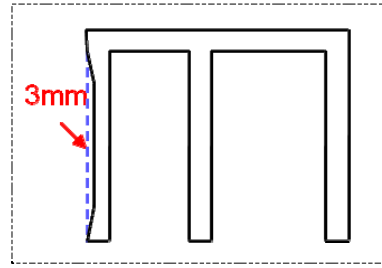


Fig. 71 pre-forming of concave pattern

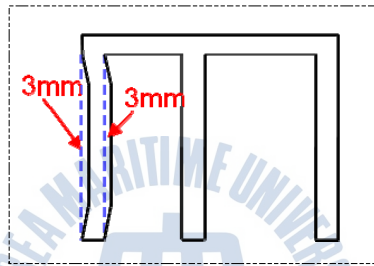


Fig. 72 Pre-forming of convex-concave pattern (A-A section)

Considering that the main thermal deformation is usually in the central area of the inner case wall, so pre-forming area is designed in the central part of the wall area.

$$L=1334\text{mm};$$

$$L_I=933\text{mm}\approx 0.7L;$$

$$W=650\text{mm};$$

$$W_I=455\text{mm}\approx 0.7W$$

4.3.2 FEM Analysis Results

The structural analysis process is as the same as previous chapters, the results are as shown in the Fig. 73~80. Table 27 lists the analysis results of pre-forming models.

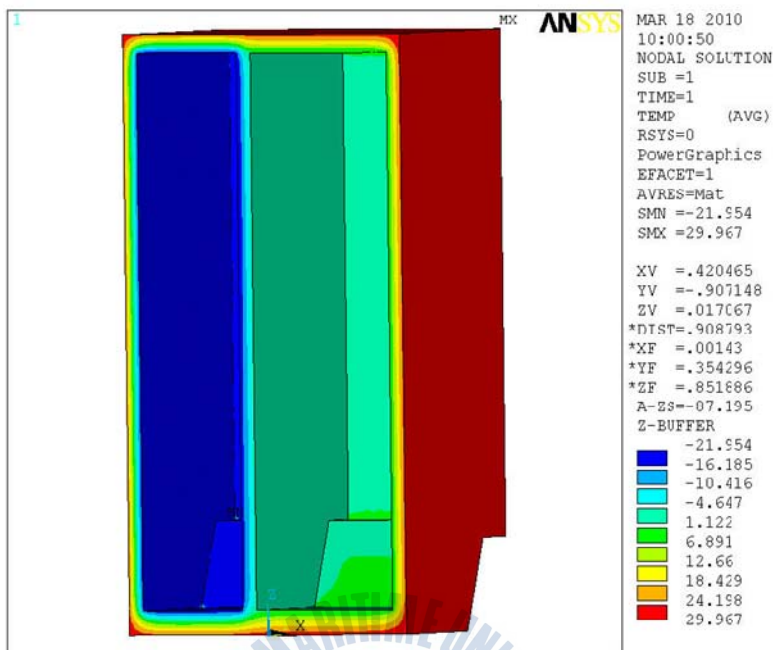


Fig. 73 Temperature distribution of smooth model

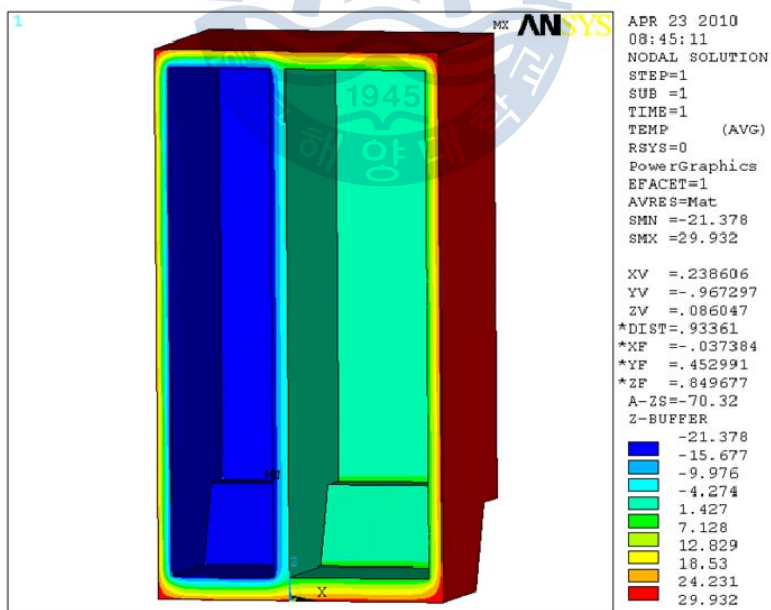


Fig. 74 Temperature distribution of convex model

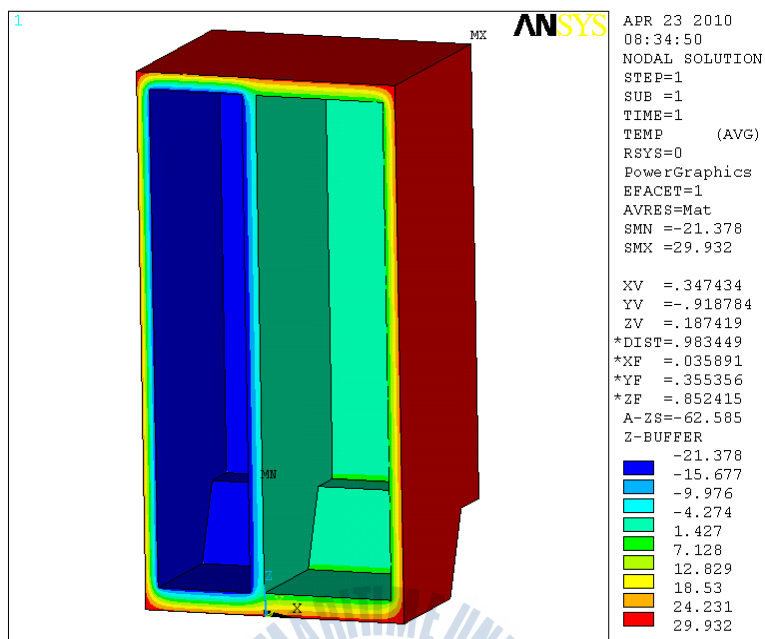


Fig. 75 Temperature distribution of concave model

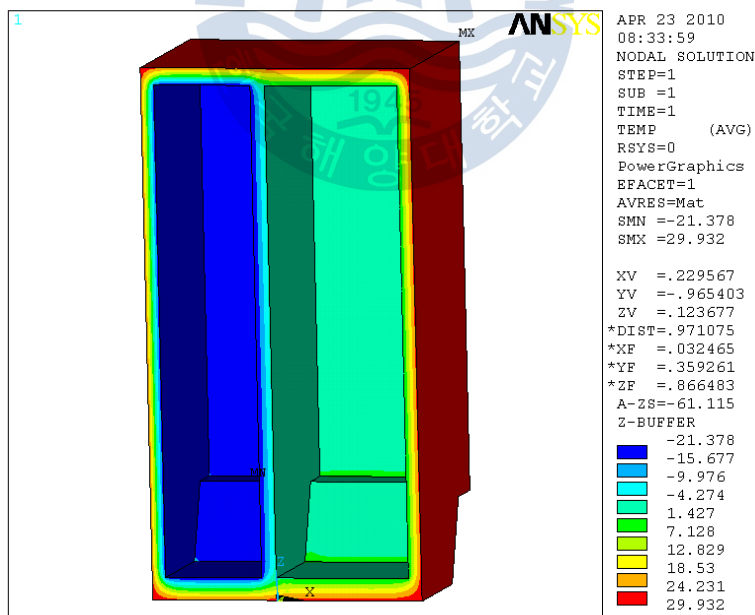


Fig. 76 Temperature distribution of convex-concave model

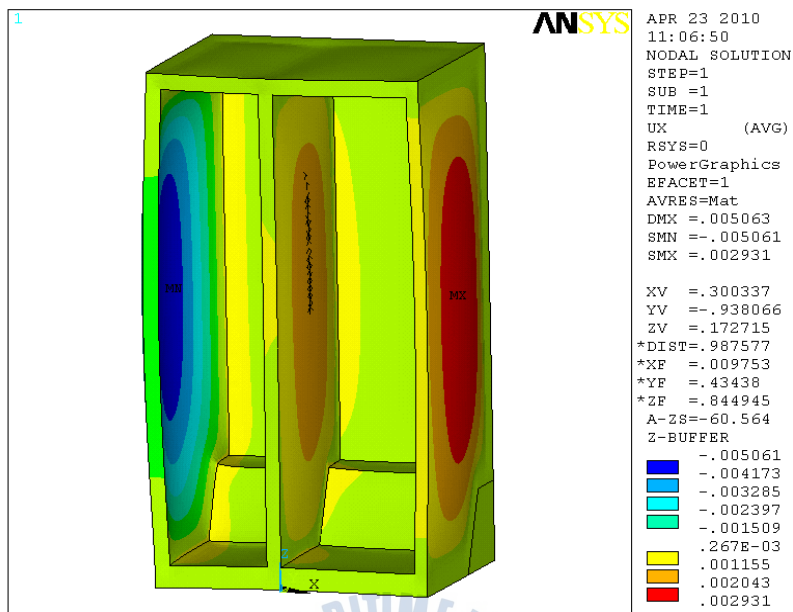


Fig. 77 Structural analysis result of smooth model

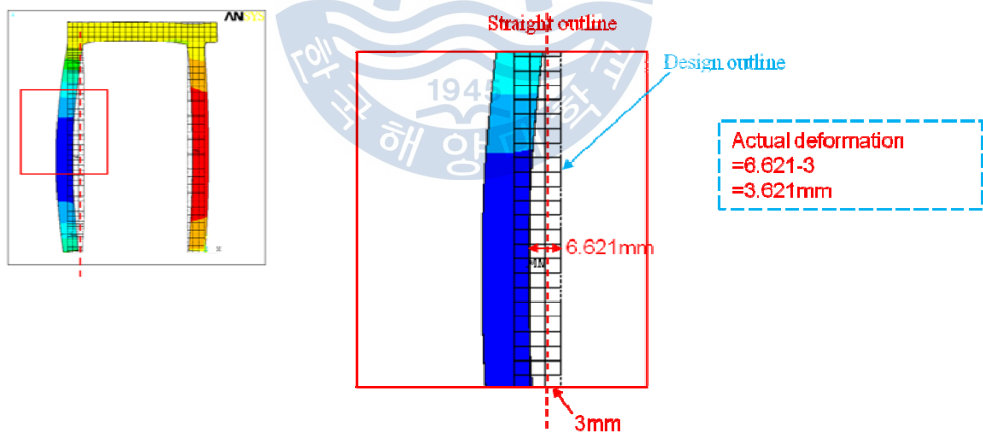


Fig. 78 Actual deformation of convex model

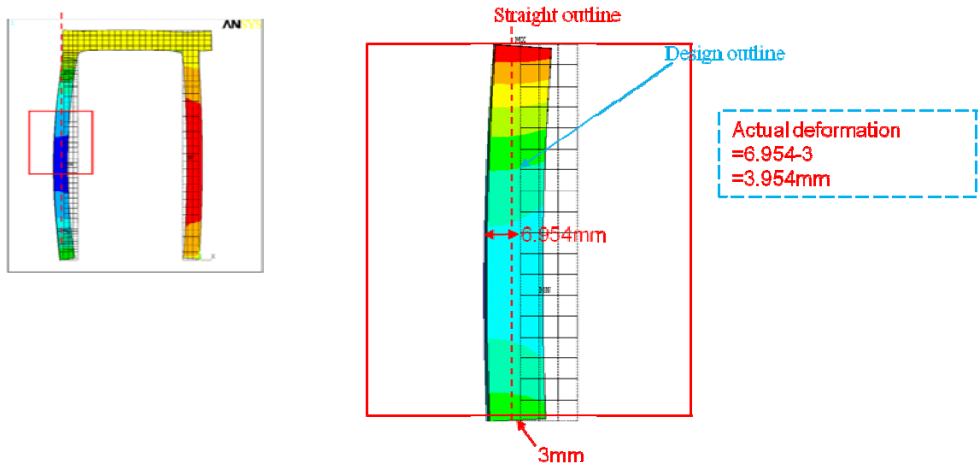


Fig. 79 Actual deformation of concave model

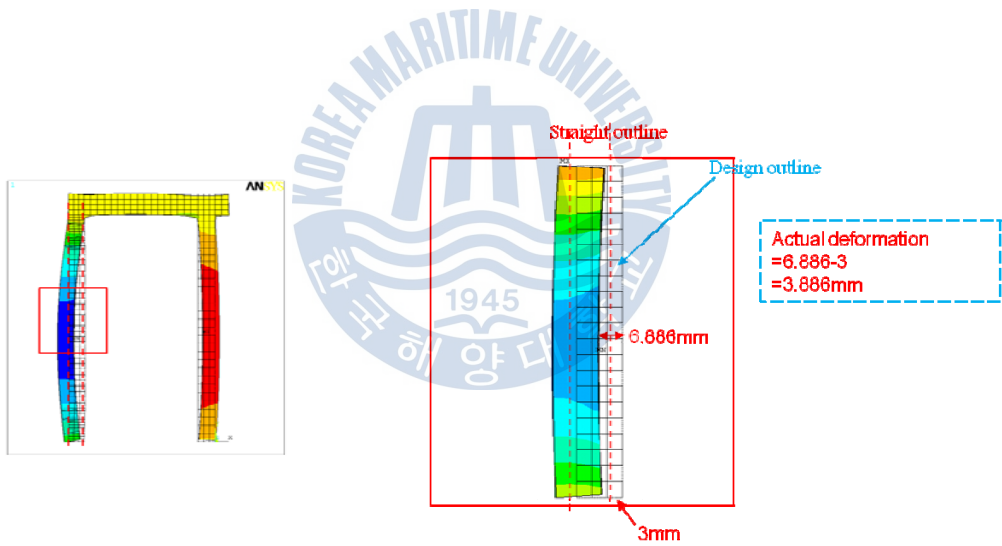


Fig. 80 Actual deformation of convex-concave model

Table 27 Analysis results of pre-forming models

Model	Actual Deformation(mm)
Smooth Model	5.063
Convex Model	6.614-3=3.614
Concave Model	6.688-3=3.886
Convex-Concave Model	6.954-3=3.954

Temperature distribution conditions are almost the same as each other of pre-forming models. The pre-formed models obviously decrease thermal deformation by means of creating pre-deformation which would make the inner case keep its ideal shape that we anticipate.



Chapter 5 Conclusion

In this paper, the FEM was applied to calculate thermal deformation of the specified refrigerator model. We developed a method of numeric analysis based on VisualBasic 6.0 combining with the APDL. A convenient interface for parameter input was developed and a thermo-mechanical analysis procedure could be carried out through dealing with VB interface realizing seamless integration for the two software and increasing analysis efficiency. We also used a method called the BP-GA method to obtain the optimal plaque parameters for minimum refrigerator inner case deformation. We designed several models with diamond shape in a hexagonal pyramid style on the inner case wall in order to analyze the cooling effect and thermal deformation. We designed several pre-forming models in order to reduce refrigerator thermal deformation effectively. The following are our conclusions:

- 1) The optimization results show that plaques had an obvious effect on refrigerator thermal bowing deformation, and the optimal plaque parameters were when plaque number was sixteen, the plaque width was about 20~25mm, depth is about 3mm, and interval distance was about 22~28mm for the refrigerator model in this study. The minimum thermal deformation was about 1.76mm.
- 2) The established ANN model was trained from thirty-eight sets of FEM analysis data and tested with an extra seven sets of FEM analysis data. The maximum test error was 7.57%. The subsequent optimal analysis using GA showed that the optimal plaque parameters were $D=2.63\text{mm}$, $W=19.24\text{mm}$, $S=49.38\text{mm}$, and minimum deformation was 1.91mm. The result of GA optimization was considered reliable, and the method for refrigerator structural optimization was practical.
- 3) The diamond pattern didn't show obvious effect on decreasing thermal deformation.

So diamond design was not suitable to decrease thermal deformation. And the diamond pattern design would increase the cost of manufacture, we don't recommend diamond pattern from the point of view of mechanical design.

4) Pre-forming models could effectively reduce refrigerator thermal deformation if parameters were designed properly. It is a new design technique worth of intensive research.



要約文

열변형을 고려한 냉장고 내벽의 구조 최적화 연구

가정용 냉장고 몸체 벽면은 강판인 외판(outer case)과 ABS 수지를 팽창성형(blow forming)하여 만든 내판(inner case)을 조립하고 그 사이에 폴리우레탄 수지를 발포시켜 구조적으로 강성을 갖도록 되어 있다. 이러한 냉장고 몸체 벽면은 다양한 재질로 인한 수축 팽창과 온도구배에 각기 다른 응답을 갖는 이종재료이다. 내벽의 ABS 는 냉장고의 차가운 격실 표면의 낮은 온도로 큰 수축을 하게 되고, 반면에 몸체 외부의 강판은 따뜻한 주변 온도에 노출되어 팽창하는 경향을 가진다. 특히 내벽의 ABS 는 두께는 1.5 mm 이고 선 팽창계수가 강판(두께 0.6 mm)에 비해서 6 배 정도로 크기 때문에 내면은 강하게 수축하면서 전체적으로 밖으로 튀어 나오는 변형(bowing)을 유도하고 자체는 큰 인장이 작용하여 균열을 일으킨다.

이러한 문제를 해결하기 위해서 냉장고 몸체에 철판을 이용한 다양한 보강재가 사용되고 있으나 이는 냉장고의 무게가 증가하고 원가가 상승하며 작업성을 나쁘게 하는 등 근본적인 문제해결 방법이 아니다. 따라서 본 논문에서는 냉장고 변형의 근본 원인이 ABS 내벽 수지의 강한 수축임을 분석하였고, 이러한 수축을 해소할 수 있도록 내벽에 함몰형 비드를 제안하여 그 효과를 해석적으로 분석하였다.

논문 2 장에서는 3 차원 해석으로 비드의 깊이에 따른 변형에 미치는 효과와 제안된 모델의 타당성을 확인하였다. 3 장에서는 비드가 포함된 내벽의 구조 최적화 연구를 2 가지 수행하였다. 첫째는 ANSYS 프로그램의 자체 최적화 기법을 도입하여 최적 비드를 설계하였으나 각 설계변수의 영향을 연속적으로 파악하기 어려웠다. 따라서 2 번째는 Artificial Neural Networks 과 Genetic Algorithm 을 사용하여 최적화 하였다. 이 2 가지 방법의 결과의 비슷하였으며 효과적인 결과를 구하였다. 4 장에서는 새로운 설계 개념을 도입하여 설계 제안을 하였으며 해석적으로 검증하였다. 다이몬드형과 같은

다각형 비드는 변형을 감소시키는 효과는 없는 것으로 분석되었고, 변형을 고려한 역변형 형상설계는 설비 보완이 이루어 지면 효과적인 방법임을 확인하였다.

본 논문은 그 동안 미흡했던 냉장고 제작에서 발생하는 변형에 대한 체계적인 연구를 수행하였으며 변형 최소화를 위한 최적화 연구를 하여 설계 방법을 제시하는데 의의가 있다.



Acknowledgements

I sincerely thank the help and efforts of everyone that has directly or indirectly helped me complete this research work. My advisor and Professor, Dr. Jong-Rae Cho has been the most influential person during the entire period of my Doctor' study and the current project. It has been a wonderful experience working with him. His tutelage has taught me more than just the required academic coursework. His technical acuity, work culture and advice are best enjoyed first-hand than when heard from others.

Secondly, I would like to express my heartfelt gratitude to Professor Ue-Kan Kim, who not only taught me a lot in vibration engineering knowledge, but also helped me so much in the life. I would like to thank Professor Dong-Hyuk Kim, Professor Jae-Hyun Jeong, Professor Hyung-Ho Jung, Professor Ildong Choi, and Professor Young-Sik Kim, who had gave me a lot of knowledge during my studying in this university. I also thank my Korean fellow students in my laboratory that helped me so much during these years.

Finally, I would like to thank my family especially my wife whose continuous love and support made it possible for me to study abroad.

Reference

1. Gary B. Jackovin, "Side-by-Side refrigeration", United States Patent 431577, 2000.
2. Muller, A.C, "Heat exchange design handbook", Hemisphere Publishing Co., New York, 1983.
3. Axel J. "Ramm, Keeping cool while cutting costs", ANSYS Advantage Excellence in Engineering Simulation, Vol.2, 2008.
4. J.W. Lord Rayleigh Strutt, "Theory of sound", Vol.1, 1877.
5. W.Ritz, "Über eine neue Methode zur Lösung gewisser Variationsprobleme der mathematischen Physik", Journal für Reine und Angewandte Mathematik, Vol.135, pp. 1–61, 1908.
6. R.Courant, "Calculus of variations and supplementary notes and exercise", Revised and Amended by Jurgen Moser, Supplementary Notes by Martin Kruskal and Hanan Rubin, Mathematics, New York University, New York, 1956–1957.
7. Clough, R.W., "The Finite element method in plane stress analysis", Proc. 2nd ASCE Conf. On Electronic Computation, Pittsburg, Pa. Sept, 1960.
8. Clough, R. W., "Original formulation of the finite element analysis", Finite Elements in Analysis and Design, Vol.7, pp.89-101, 1991.
9. MSC/PATRAN Graphics and finite element package. Vols. II and I. The MacNeal-Schwendler Corporation, Costa Mesa, California, 1997.
10. Turner, M.J., Clough, R.W., Martin, H.C., Topp, L.J., "Stiffness and deflection analysis of complex structures", J. Aero. Sci., Vol.23, pp.805-824, 1956.
11. Argyris, J., Kelsey, S., "Energy theorems and structural analysis", Butterworths, London, 1960.

12. A.S. Usmani*, J.M. Rotter, S.Lamont, A.M. Sanad, M.Gillie, “Fundamental principles of structural behavior under thermal effects”, Journal of Fire Safety, Vol.36, pp.721-744, 2001.
13. Williams, S.G. and Schwartz, D.L., “Method and apparatus for manufacture of plastic refrigerator liners”, US Patent 5269601, 1993.
14. Vanderplaats GN. “Numerical optimization techniques for engineering design”. McGraw-Hill Inc, pp.250-82, 1984.
15. ANSYS V5.6 User Manual, ANSYS Inc., Southpointe, 275 Technology Drive, Canonsburg, PA 15317, USA.
16. Vanderplaats GN, Salajegheh E. “A new approximation method for stress constraints in structural synthesis”, AIAAJ, Vol.27, No.3, pp.352-358, 1989.
17. Hansen SR, Vanderplaats GN, “Approximation method for configuration optimization of trusses”. AIAA J, Vol.28, No.1, pp.161-168, 1990.
18. Schmit LA, Miura H. “Approximation concepts for efficient structural synthesis”, NASA CR-2552, 1975.
19. Imai K. “Configuration optimization of trusses by the multiplier method”, Mechanics and Structures Department, School of Engineering and Applied Science. University of California, Los Angeles, Report No. UCLA-Eng-7842, 1978.
20. Ashok D. Belegundu, Jasbir S. Arora, “A study of mathematical programming methods for structural optimization”, International Journal for Numerical Methods in Engineering, Vol.21, Issue 9, pp.1583-1599, 1985.
21. Qian LX, Zhang WX, Siu YK, Zhang JT. “Efficient optimum design of structures-program DDDU”, Computer Methods in Applied Mechanics and Engineering. Vol.30, No.2, pp.209-224, 1982.

22. Hall SK, Cameron GE, Grierson DE. "Least weight design of steel frameworks accounting for PA effects", Journal of Structure Engineering. ASCE, Vol.115, No.6, pp.1463-1475, 1989.
23. Erbatur F, Al-Hussainy MM. "Optimum design of frames". Computers and Structures, Vol.45, pp.887-891, 1992.
24. Gellatly RA, Berke L. "Optimal structural design", Report No. AFFDL-TR-70-165, Air Force Flight Dynamics Laboratory, Wright-Patterson Air force Based, Ohio, 1971.
25. Venkayya VB. "Design of optimum structures". Computers and Structures, Vol.1, pp.265-309, 1971.
26. Allowood RJ, Chung YS. "Minimum-weight design of trusses by an optimality criteria method". Numerical Methods in Electromagnetism, Vol. 20, pp.697-713, 1984.
27. Kirsch U. "Feasibility and optimality in structural design". Computers and structures, Vol.41, No.6, pp.1394-1456, 1991.
28. Chang KJ. "Optimality criteria methods using K-S functions". Structural Optimization Vol.4, No. 3-4, pp.213-217 1992.
29. Rozvany GIN, Zhou M. "Continuum based optimal criteria (COC) methods: an introduction in optimization of large structural systems". Proceedings of the NATO/DFGASI, Berchtesgaden. Dordrecht, The Netherlands:Kluwer, pp.1-26, 1993.
30. Erbatur F, Hasancebi O, Tutuncu I, Kilic H. "Optimal design of planar and space structures with genetic algorithms". Computers and Structures, Vol.75, pp.209-224, 2000.
31. J.H.Holland, Adaptation in Natural and Artificial Systems: An Introductory Analysis with Applications to biology, control and artificial intelligence. MIT Press, ISBN 0-262-581116, 1998. (NB Original printing 1975).
32. Goldberg DE, Samtani MP. "Engineering Optimization via the genetic algorithm". 9th Conference on Electronic Computation, New York, ASCE, pp.471-482, 1986.

33. Goldberg DE. "Genetic algorithms in search, optimization and machine learning". Reading, MA: Addison-Wesley, 1989.
34. Felix JE. "Shape Optimization of Trusses Subject to Strength, Displacement, and Frequency Constraints". Masters Thesis, Naval Postgraduate School, 1981.
35. Hajela P, Shih CJ. "Multi-objective optimum design in mixed integer and discrete design variable problems". AIAA, Vol.118, No.4, pp.670-675, 1990.
36. Rajan SD. "Sizing, shape, and topology design optimization of trusses using genetic algorithms". Journal of Structural Engineering Vol.121, No.10, pp.1480-1487, 1995.
37. Rajeev S, Krishnamoorthy CS. "Discrete optimization of structures using genetic algorithms". Journal of Structural Engineering, Vol.118, No.5, pp.1233-1250, 1992.
38. Deb K, Gulati S. "Design of truss-structures for minimum weight using genetic algorithms". Finite Elements Anal Design, Vol.37, pp.447-465, 2001.
39. Nicholas Ali, Kamran Behdinan, Zouheir Fawaz. "Applicability and viability of a GA based finite element analysis architecture for structural design optimization". Vol.81, Issues 22-23, pp.2259-2271, 2003.
40. George F.Luger. "Artificial Intelligence: Structures and strategies for complex problem solving". Beijing Mechanic Industry Press, 2003.
41. Xiaodong, Ge, "VB.NET programming examples and techniques". Beijing Hope Electronic Press, pp.1-2, 2003.
42. Shao Jun, Xiang Zong-fang, Wang Ping, "Development technology of ANSYS based on VB". Journal of Chongqing Vocational & Technical Institute, Vol.15, No.2, pp.144-145, 2006.
43. Luo Ming, "On the application of VB in the ANSYS redevelopment". Journal of Tianjin Vocational Institutes, Vol. 8, No. 5, pp.53-56, 2006.
44. "MATLAB's User Guide". The Math Works Inc., 3 Apple Hill Drive, Natick, MA,

1999.

45. LIN Gao-yong, ZHOU Jia, ZHANG Yong-ning, CHEN Xing-ke, JIANG Jie, WANG Fang, "Optimization of deflector hole for aluminum profile extrusion die". J.Cent.South Univ, Vol.38, No.2, pp.225-231, 2007.

46. Ming-Jong Tsai, Chen-Hao Li, Cheng-Che Chen, "Optimal laser-cutting parameters for QFN packages by utilizing artificial neural networks and genetic algorithm". Journal of Materials Processing Technology, Vol.208, pp.270-283, 2008.

47. Chung, J.S., Hwang, S.M., 1997. "Application of a genetic algorithm to the optimal design of the die shape in extrusion". Journal of Material Processing Technology, Vol.72, pp.69-77, 1997.

48. Badran, S.M., Al-Duwaish, H.N., "Optimal output feedback controller based on genetic algorithms". Electric Power Systems Research, Vol.50, pp.7-15, 1999.

49. Huang, W., Lam, H.N., "Using genetic algorithms to optimize controller parameters for HVAC", Energy Building Vol 26, pp.277-282, 1997.

50. PATANKAR S V, LIU C H and SPARROW EM, "Fully developed flow and heat transfer in ducts having streamwise periodic variations of cross sectional area". Journal of Heat Transfer, Vol.99, pp. 180-186, 1977.

51. LIU Zhen-yan, LIU Zhen-yi, SONG Ji-tian, WANG Hong-ling. "Study on Heat Transfer Mechanism and Characteristics of Concave and Raised Surface". Journal of Energy Conservation Technology, Vol.25, No.144, pp.305-308, 2007.